ACCSCIENCE PUBLISHING

Innovative Medicines & Omics

ORIGINAL RESEARCH ARTICLE

# Evaluation of the nephroprotective potential of chrysin against pentadecafluorooctanoic acid-induced kidney dysfunction in male Wistar rats

**Adeoye B. Awolesi*, Tomisin M. Koledoye, Rereloluwa M. Adesina, Kikelomo C. Omoniyi, and Stephen A. Praise**

Department of Biochemistry, College of Biosciences, Federal University of Agriculture, Abeokuta, Ogun State, Nigeria

## Abstract

Pentadecafluorooctanoic acid (PFOA) is a highly persistent environmental contaminant known for its bioaccumulative nature and ability to cause adverse renal effects. Prolonged exposure to PFOA has been associated with oxidative stress, inflammation, and membrane dysfunction, which collectively contribute to renal impairment. This study investigates the nephroprotective effects of chrysin, a naturally occurring flavonoid with potent antioxidant and anti-inflammatory properties, against PFOA-induced kidney toxicity in male Wistar rats. Twenty-five rats were divided into five groups ($n$ = 5 per group): (i) control (20% dimethyl sulfoxide), (ii) PFOA-only (5 mg/kg), (iii) 25 mg/kg chrysin + 5 mg/kg PFOA, (iv) 50 mg/kg chrysin + 5 mg/kg PFOA, and (v) 50 mg/kg chrysin-only. All treatments were administered orally for 14 consecutive days. Exposure to PFOA resulted in a significant ($p < 0.05$) elevation in serum creatinine, lactate dehydrogenase, and electrolyte imbalances, accompanied by reduced antioxidant enzyme activities, elevated oxidative stress markers, increased inflammatory cytokines, and disrupted ATPase activity. Chrysin pre-treatment at both 25 and 50 mg/kg markedly attenuated these toxic effects in a dose-dependent manner. It restored antioxidant defenses, normalized biochemical indices, improved electrolyte balance, and suppressed inflammation, thereby preserving renal function. These findings suggest that chrysin confers significant nephroprotective effects against PFOA-induced renal injury by mitigating oxidative stress, inflammation, and ion transport disruption, supporting its therapeutic potential as a promising nephroprotective agent for protecting against environmentally induced kidney injury.

***Keywords:*** Chrysin; Pentadecafluorooctanoic acid; Oxidative stress; Nephroprotective; Kidney dysfunction

***Corresponding author:**
Adeoye B. Awolesi
(Awolesiadeoye1@gmail.com)

**Citation:** Awolesi AB, Koledoye TM, Adesina RM, Omoniyi KC, Praise SA. Evaluation of the nephroprotective potential of chrysin against pentadecafluorooctanoic acid-induced kidney dysfunction in male Wistar rats. *Innov Med Omics*. doi: 10.36922/IMO026250043

**Received:** June 16, 2026

**Revised:** June 29, 2026

**Accepted:** July 2, 2026

**Published online:** July 16, 2026

**Copyright:** © 2026 Author(s). This is an Open-Access article distributed under the terms of the Creative Commons Attribution License, permitting distribution, and reproduction in any medium, provided the original work is properly cited.

**Publisher's Note:** AccScience Publishing remains neutral with regard to jurisdictional claims in published maps and institutional affiliations.

## 1. Introduction

Chrysin, a natural flavonoid found abundantly in honey and propolis, has attracted considerable attention for its diverse pharmacological properties, including antioxidant, anti-inflammatory, and anti-apoptotic effects.[1-3] Preclinical studies have demonstrated its nephroprotective role in models of drug-induced renal injury. For example, in cisplatin-induced nephrotoxicity, chrysin restored glutathione (GSH) levels, suppressed nuclear

factor κ-light-chain-enhancer of activated B cells (NF-κB)-mediated inflammation, and improved renal function.[4,5] Similarly, in adenine-induced chronic kidney disease, it reduced oxidative stress and ameliorated histopathological damage.[3,6] Evidence from cyclosporine-A–induced renal fibrosis models further highlights chrysin's potential, showing that it inhibited inflammatory signaling and preserved kidney architecture.[7,8]

Despite these promising findings, chrysin's efficacy against environmental toxicants such as pentadecafluorooctanoic acid (PFOA) remains largely unexplored. This gap is critical, given that PFOA—also known as perfluorooctanoic acid—is a persistent environmental pollutant that induces nephrotoxicity through mechanisms distinct from those involved in chemotherapeutic- or drug-induced injuries. These mechanisms include mitochondrial dysfunction, aquaporin downregulation, and disruption of redox homeostasis.[9–12] Recent studies by Rashid *et al.*[12], Ma *et al.*[13], and Zou *et al.*[14] implicate the nuclear factor erythroid 2-related factor 2 (Nrf2) pathway and the nucleotide-binding oligomerization domain-like receptor protein 3 (NLRP3) inflammasome as central mediators of PFOA-induced renal damage, highlighting them as potential therapeutic targets for flavonoid-based interventions.

Notably, chrysin has been reported to activate Nrf2-dependent antioxidant responses in cadmium-induced nephrotoxicity, enhancing heme oxygenase-1 (HO-1) expression and reducing lipid peroxidation.[3,15] In parallel, its suppression of the NLRP3 inflammasome activation has been linked to attenuation of inflammatory cytokine release and renal fibrosis in cyclosporine-A models.[7,8] These mechanisms overlap with PFOA's toxicological profile, which involves exacerbation of oxidative DNA damage and impairment of mitochondrial redox balance.[12] Thus, by targeting the Nrf2 and NLRP3 pathways, chrysin may represent a potential dual protective strategy against both oxidative stress and inflammatory signaling associated with PFOA exposure.[16]

To our knowledge, this study is the first to investigate the nephroprotective potential of chrysin against PFOA-induced renal injury in male Wistar rats. We hypothesize that chrysin will mitigate PFOA toxicity by enhancing antioxidant defenses, suppressing pro-inflammatory cytokines and myeloperoxidase (MPO) activity, and restoring membrane-bound ATPase function, as supported by Chen *et al.*[7] Additionally, the study will assess chrysin's impact on nitric oxide (NO) depletion, lipid peroxidation (as indicated by malondialdehyde [MDA]), reduced GSH, and biochemical markers of renal dysfunction such as serum creatinine, lactate dehydrogenase (LDH), and electrolyte imbalances. By integrating these endpoints, this research provides a comprehensive multi-target evaluation of chrysin's protective mechanisms and its potential as a therapeutic agent against PFOA-induced nephrotoxicity.

## 2. Materials and methods

### 2.1. Chemicals and reagents

Pentadecafluorooctanoic acid was purchased from Sigma-Aldrich (USA). Chrysin and dimethyl sulfoxide (DMSO) were obtained from Otto Chemical Pvt. Ltd. (India). SPECTRUM diagnostic kits for electrolyte analysis, including sodium (No. 303001), potassium (No. 298001), calcium (No. 226001), and magnesium (No. 285001), as well as creatinine, were purchased from Obour City Industrial Area (Egypt). Interferon (IFN)-γ (E-EL-R0009) and interleukin (IL)-1β (E-EL-R0012) ELISA kits were procured from ElabScience (USA). Total protein assay kits (TP245) were purchased from Randox Laboratories Ltd. (United Kingdom). The Griess reagent kit (No. 780001) was obtained from Cayman Chemical (USA).

Sodium pyruvate, nicotinamide adenine dinucleotide (NADH), sodium ethylenediaminetetraacetic acid, hydrogen peroxide ($H_2O_2$), sodium azide, 2-thiobarbituric acid (TBA), ascorbic acid, trichloroacetic acid (TCA), sodium hydroxide, dipotassium hydrogen phosphate, potassium dihydrogen phosphate, potassium chloride (KCl), magnesium chloride ($MgCl_2$), sodium chloride (NaCl), disodium ATP, reduced GSH, oxidized GSH (GSSG), 1-chloro-2,4-dinitrobenzene (CDNB), Ellman's reagent (5,5'-dithiobis[2-nitrobenzoic acid]; DTNB), pyrogallol, hydrazine sulfate, sulfuric acid ($H_2SO_4$), and ammonium molybdate were procured from Sigma-Aldrich (USA). $H_2SO_4$ was also supplied by Ajax Finechem (Australia), while sodium dodecyl sulfate (SDS) was purchased from British Drug Houses (United Kingdom). Unless otherwise stated, all other reagents used were of analytical grade.

### 2.2. Experimental animals

A total of 25 male Wistar rats weighing 120–180 g were procured and housed in well-ventilated cages at the Animal House, Department of Biochemistry, College of Biosciences, Federal University of Agriculture, Abeokuta. The animals were acclimatized for 14 days prior to the experiment and maintained on a standard diet with water provided *ad libitum*. All procedures complied with institutional and international ethical standards for the use of laboratory animals in research. All animals were handled and cared for in accordance with the *Guide for the Care and Use of Laboratory Animals* and the ARRIVE

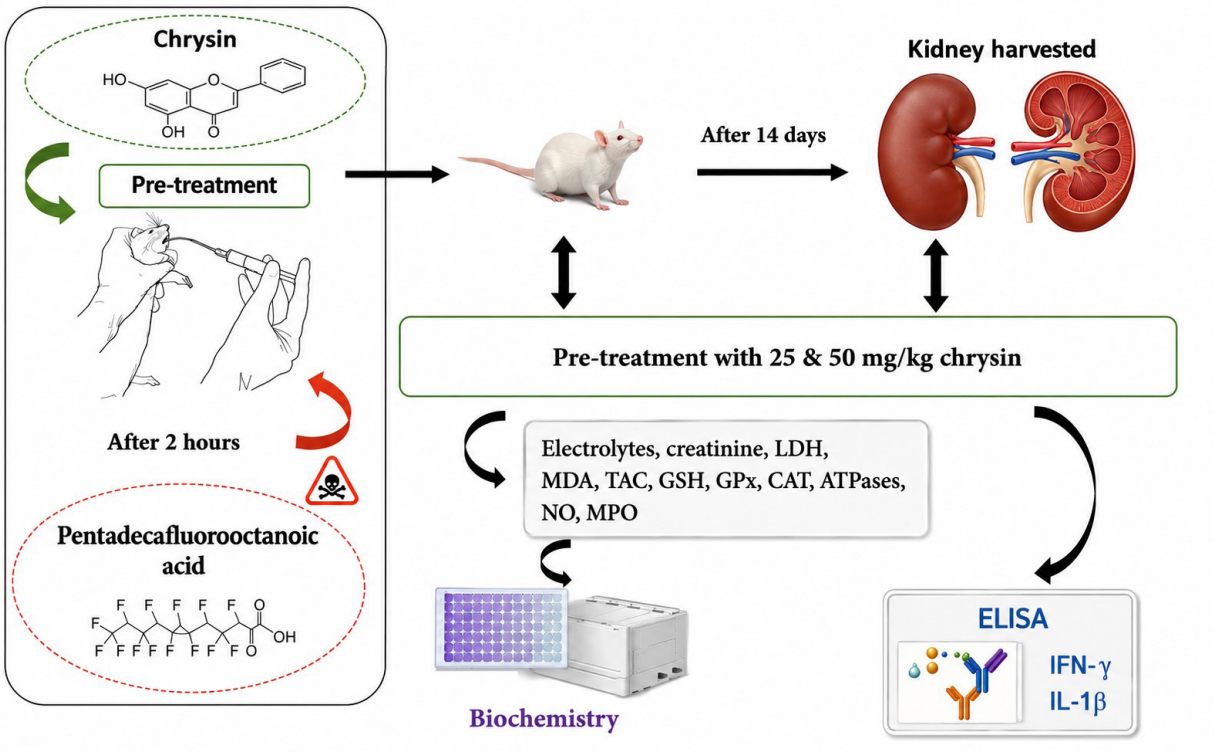


**Figure 1.** Schematic of the experimental design. Twenty-five male Wistar rats were randomly assigned to five groups: control (20% dimethyl sulfoxide; vehicle control), PFOA-only, PFOA + 25 mg/kg chrysin, PFOA + 50 mg/kg chrysin, and 50 mg/kg chrysin-only. Following a two-week acclimatization period, the animals received treatments for two weeks. The selected doses of PFOA and chrysin were based on preliminary pilot studies and previous reports.[17–26]

Abbreviations: CAT: Catalase; ELISA: Enzyme-linked immunosorbent assay; GPx: Glutathione peroxidase; GSH: Glutathione; IFN: Interferon; IL: Interleukin; LDH: Lactate dehydrogenase; MDA: Malondialdehyde; MPO: Myeloperoxidase; NO: Nitric oxide; TAC: Total antioxidant capacity.

guidelines.[27,28] Ethical approval for this study was obtained from the Federal University of Agriculture, Abeokuta Ethical Committee (approval no. FUNAAB/COLBIOS/BCH/UG/20191153).

### 2.3. Experimental design

Following a two-week acclimatization period, 25 male Wistar rats were randomly divided into five groups, with five animals in each group ($n$ = 5). Treatments were administered orally for 14 consecutive days. Prior to administration, chrysin and PFOA were dissolved in 20% DMSO to prepare the working solutions.[17,29–32] A 20% DMSO solution was selected as the common vehicle because it effectively dissolved both PFOA and chrysin, and the vehicle control group received the same formulation without the test compounds to account for any potential effects of the solvent.[18–20] Animals received daily oral doses of chrysin (25 or 50 mg/kg body weight) or PFOA (5 mg/kg body weight) via oral gavage. The selected chrysin doses have previously been reported to attenuate renal injury, oxidative stress, and inflammation in rats[3,22–26], whereas the 5 mg/kg dose of PFOA is known to induce oxidative stress, inflammation, and renal toxicity.[33–35] Group allocations, including the normal control (I) and treatment groups (II–V), are presented in Table 1. In the pre-treatment groups (III and IV), chrysin was administered first, followed by a single oral dose of PFOA 2 h later, to enhance chrysin bioavailability as illustrated in Figure 1.

### 2.4. Sample collection

On the 14th day of administration, animals were fasted overnight, after which blood was collected via ocular puncture from the retro-orbital plexus and transferred into pre-labeled plain tubes. The samples were centrifuged at 3,500 rpm for 10 min at 4 °C to obtain serum, which was stored at −4 °C for subsequent biochemical analyses. The animals were then humanely euthanized by cervical dislocation, and the kidneys were harvested, rinsed in ice-cold phosphate-buffered saline (pH 7.4), weighed, and processed for homogenization.[36,37]

**Table 1. Animal grouping and treatment regimen**

| Experimental groups (*n* = 5) | Treatment (oral, 14 days) |
|---|---|
| Control | 20% DMSO |
| PFOA-only | 5 mg/kg PFOA |
| 25 mg/kg chrysin + PFOA | 25 mg/kg chrysin + 5 mg/kg PFOA (2 h apart) |
| 50 mg/kg chrysin + PFOA | 50 mg/kg chrysin + 5 mg/kg PFOA (2 h apart) |
| Chrysin-only | 50 mg/kg chrysin |

Abbreviations: DMSO: Dimethyl sulfoxide; PFOA: Pentadecafluorooctanoic acid.

## 2.5. Homogenate preparation and biochemical assays

Renal cortical tissues were processed as 10% (w/v) homogenates to obtain cell-free supernatants for biochemical analyses. Briefly, 0.2 g of fresh kidney cortex was weighed and homogenized in 1.8 mL of ice-cold 0.1 M phosphate-buffered saline (pH 7.4) using a motor-driven Teflon-glass homogenizer (Thomas Scientific, USA) to ensure efficient cell disruption, as described by Hasim *et al.*[38] The homogenates were centrifuged at 4,000 × g for 10 min at 4 °C, and the resulting supernatants were collected, aliquoted, and stored at −80 °C until further biochemical assays.[39–41] Protein concentrations in serum and tissue homogenates were determined spectrophotometrically using the Lowry method[42], with bovine serum albumin (Randox Laboratories Ltd., United Kingdom) as the standard, according to the Randox total protein assay kit protocol.[43] Enzyme activities were normalized to protein content to account for sample variability.

### *2.5.1. Creatinine estimation and lactate dehydrogenase activity*

Creatinine concentration in kidney tissue homogenates and serum was quantified using a SPECTRUM creatinine assay kit according to the manufacturer's protocol. This optimized kinetic method utilizes an improved Jaffe reaction, wherein creatinine reacts with picric acid in alkaline solution to form a colored complex, with proprietary modifications to enhance specificity and reduce interference from non-creatinine chromogens. The assay was performed by adding 100 µL of sample to 1.0 mL of working reagent (containing 25 mM picric acid and 0.4 mol/L sodium hydroxide). The solution was mixed thoroughly, and after exactly 30 s, the initial absorbance ($A_1$) was measured at 492 nm against a reagent blank. After exactly 2 min, the final absorbance ($A_2$) was measured. The change in absorbance ($\Delta A = A_2 - A_1$) was used to calculate creatinine concentration based on the kit's certified standard. Results for kidney tissue were normalized to tissue weight and expressed as µmol/g tissue, while serum results were expressed as µmol/L.

Lactate dehydrogenase activity was determined spectrophotometrically according to Holmes and Scopes[44], as modified by Al-Jassabi[45] by monitoring the enzyme-catalyzed reaction: pyruvate + NADH + $H^+$ → L-lactate + $NAD^+$. The assay was initiated by adding a 20 µL aliquot of sample to 1 mL of a reaction mixture consisting of 50 mM potassium phosphate buffer (pH 7.5), 0.18 mM NADH, and 0.6 mM sodium pyruvate, pre-equilibrated to 30 °C. The decrease in absorbance at 340 nm, resulting from the oxidation of NADH, was monitored kinetically. LDH activity was calculated from the maximum linear rate of change in absorbance ($\Delta A_{340}$/min) using the formula:

$$Activity\ (U/g) = \frac{\Delta A340/min \times dilution\ factor}{6.22} \quad (1)$$

where the divisor of 6.22 is derived from the molar extinction coefficient for NADH (ε = 6,220 $M^{-1}$ $cm^{-1}$). Activity was expressed as units per gram of protein (U/g), with one unit defined as the amount of enzyme that oxidizes 1 µmol of NADH per minute under the assay conditions.

### *2.5.2. Electrolyte analysis*

Electrolyte concentrations, including sodium, potassium, calcium, and magnesium, were determined in serum and kidney homogenates using commercial SPECTRUM diagnostic kits, according to the manufacturer's recommended colorimetric protocols. Sodium levels were measured based on the selective chromogen principle, which generates a chromophore with absorbance proportional to sodium concentration, measured at 630 nm and expressed as mEq/L. Potassium levels were assayed using the turbidimetric tetraphenylborate method, where potassium ions form a stable turbid complex with tetraphenylborate at alkaline pH. The resulting turbidity was quantified at 578 nm, with concentrations expressed as mmol/L. Calcium levels were assessed using the O-cresolphthalein complexone method, which produces a violet-colored complex measurable at 578 nm. Concentrations were expressed as mg/dL. Magnesium was analyzed using the phosphonazo III endpoint method, in which magnesium ions form a colored chelate complex, measured spectrophotometrically at 630 nm. Calcium interference was eliminated by chelation with ethylene glycol tetraacetic acid. Magnesium concentrations were expressed as mg/dL.

#### *2.5.3. Oxidative stress biomarkers*

Malondialdehyde, a well-established marker of lipid peroxidation, was quantified using the thiobarbituric acid-reactive substances (TBARS) method.[46] Under acidic conditions, MDA reacts with TBA to form a pink chromophore, measurable at 532 nm. This method, originally described by Buege and Aust[47] and later optimized by Hodges *et al.*[46], was employed for kidney homogenate analysis.

Briefly, 0.5 mL of sample (or distilled water as the blank) was mixed with 1.0 mL of TBARS reagent containing 15% TCA, 0.37% TBA, and 0.25 M hydrochloric acid (HCl; 1:1:1, v/v/v). The mixture was incubated in a boiling water bath at 98 °C for 15 min, then rapidly cooled on ice. Following centrifugation at 3,500 rpm for 10 min, the absorbance of the supernatant was recorded at 532 nm against the blank. TBARS levels were expressed as nmol MDA/g tissue, using the molar extinction coefficient (ε) of $1.56 \times 10^5$ $M^{-1}$ $cm^{-1}$ with a 1 cm path length.

Reduced GSH levels were quantified using Ellman's reagent (DTNB), which reacts with thiol groups to yield the yellow chromophore 2-nitro-5-thiobenzoate (TNB).[48] The absorbance of TNB was recorded spectrophotometrically at 412 nm, as described by Ellis.[49] Briefly, kidney tissue homogenates were mixed with 25 µL of 10% TCA and centrifuged at 4,000 rpm for 5 min. The resulting supernatant (34 µL) was transferred to fresh Eppendorf tubes and combined with 350 µL of GSH working reagent (prepared by mixing 68.63 mL of GSH buffer with 1.37 mL of 1 mM DTNB solution). After incubation at room temperature for 10 min, absorbance was measured at 412 nm. GSH concentration was calculated in µmol/mg protein using a molar extinction coefficient (ε) of $14.15 \times 10^3$ $M^{-1}$ $cm^{-1}$ and a path length of 1 cm.

#### *2.5.4. Antioxidant enzyme biomarkers and total antioxidant capacity*

Superoxide dismutase (SOD) activity was determined based on its ability to inhibit pyrogallol autoxidation.[50] The reaction was monitored spectrophotometrically at 420 nm. Specifically, renal SOD activity was assayed by evaluating the inhibition of pyrogallol autoxidation, a superoxide-reactive indicator molecule that competes with SOD for superoxide radicals in an alkaline medium (pyrogallol/SOD + $O_2\bullet^- + 2H^+ \rightarrow H_2O_2 + O_2$), as described by Marklund and Marklund.[51] Briefly, the reaction mixture consisted of the sample (or distilled water as the blank) combined with Tris-HCl buffer (180 µL, 50 mM, pH 8.2) containing 1 mM ethylenediaminetetraacetic acid. After thorough mixing, 250 µL of distilled water was added, and the mixture was incubated for 10 min at room temperature. The reaction was then initiated by adding pyrogallol (50 µL, 1 mM). The rate of pyrogallol autoxidation was monitored by measuring absorbance changes at 420 nm every 30 s for 3 min. SOD activity was expressed as U/mg protein using the pyrogallol molar absorption coefficient (ε) of $8.0 \times 10^5$ $M^{-1}$ $cm^{-1}$.

Catalase (CAT) activity was determined spectrophotometrically by measuring the enzyme's catalytic decomposition of $H_2O_2$ into water and oxygen ($2H_2O_2 \rightarrow 2H_2O + O_2$), as described by Shangari and O'Brien.[52] The assay is based on the reaction of ammonium orthomolybdate with undecomposed $H_2O_2$ to form a stable yellow complex.

Briefly, a sample aliquot was mixed with 1.0 mL of substrate solution (65 µM $H_2O_2$ in 60 mM sodium-potassium phosphate buffer, pH 7.4) and incubated at 37 °C for 60 s. The reaction was terminated by adding 1.0 mL of 32.4 mM ammonium orthomolybdate. Two control reactions were included: one containing $H_2O_2$ substrate and phosphate buffer without sample (to account for non-enzymatic $H_2O_2$ decomposition), and another containing sample and phosphate buffer without $H_2O_2$ (to account for sample chromogenicity). The absorbance of the yellow molybdate–$H_2O_2$ complex was recorded at 405 nm. CAT activity, proportional to the decrease in $H_2O_2$ concentration, was calculated using the $H_2O_2$ molar extinction coefficient (ε) of 43.6 $M^{-1}$ $cm^{-1}$. Specific activity was expressed as kilounits per milligram of protein (kU/mg protein).

Glutathione peroxidase (GPx) activity was assayed using a coupled enzymatic reaction as described by Rotruck *et al.*[53] The assay quantifies the enzyme's catalytic activity, where GPx reduces $H_2O_2$ while oxidizing reduced GSH to its oxidized form (GSSG), as shown in the reaction: $H_2O_2 + 2GSH \rightarrow GSSG + 2H_2O$. The activity was determined by measuring the consumption of GSH during the reaction.

Briefly, a sample aliquot was mixed with 75 µL of GPx working reagent (containing 2.5 mM $H_2O_2$, 4 mM GSH, and 10 mM sodium azide to inhibit CAT activity) in a dedicated GPx buffer and incubated at 37 °C for 5 min. The reaction was terminated by adding 25 µL of 10% (w/v) TCA to precipitate proteins. The mixture was then centrifuged at 4,000 rpm for 5 min to pellet the precipitate. Subsequently, 34 µL of the clear supernatant was carefully transferred to a fresh tube. Then, 350 µL of GSH working reagent (DTNB in buffer) was added. This mixture was incubated at 37 °C for 10 min to allow the DTNB to react with any residual GSH, producing the yellow-colored TNB anion. The absorbance of this TNB chromophore was measured spectrophotometrically at 412 nm. Since GPx activity is inversely proportional to the amount of residual

GSH remaining after the initial incubation period, the decrease in absorbance correlates directly with higher GPx activity. Specific activity was calculated using the molar extinction coefficient (ε) for TNB of 14,150 $M^{-1}$ $cm^{-1}$ and a path length of 1 cm. Results were expressed as U/mg protein.

Glutathione S-transferase (GST) activity was determined spectrophotometrically using the method established by Habig *et al.*[54], which exploits the enzyme's catalytic conjugation of reduced GSH with the substrate CDNB. This reaction yields a sharp increase in absorbance as the GS–DNB conjugate forms, releasing a proton in the process (GSH + CDNB → GS–DNB + $H^+$ + $Cl^-$).

For the assay, each sample was introduced into a prepared reaction mixture containing 2.5 mL of 0.1 M phosphate buffer (pH 6.5), 0.1 mL of GSH solution, and 0.1 mL of CDNB solution, as described by Tew and Ronai.[55] The kinetic progression of the reaction was immediately monitored by measuring the increase in absorbance at 340 nm every 30 s over a 3-min period in a temperature-controlled spectrophotometer. GST specific activity was quantified from the linear rate of absorbance product formation using a molar extinction coefficient (ε) of 9.6 $mM^{-1}$ $cm^{-1}$ for the GS–DNB conjugate and normalized to total protein content, with results expressed as U/mg of protein.

Total antioxidant capacity (TAC) was quantified using the phosphomolybdenum reduction assay as described by Prieto *et al.*[56] This method is based on the reduction of Mo(VI) to Mo(V) by antioxidants present in the sample, resulting in the formation of a green phosphate-Mo(V) complex with a characteristic absorption maximum. Briefly, 0.1 mL of sample was combined with 1 mL of reagent solution (containing 0.6 M $H_2SO_4$, 28 mM sodium phosphate, and 4 mM ammonium molybdate) in a 1.5 mL microcentrifuge tube. The tubes were tightly capped and incubated in a thermal block at 95 °C for 90 min to facilitate color development. After incubation, the samples were cooled to room temperature and centrifuged at 1,500× *g* for 5 min to pellet any particulate matter. The absorbance of the resulting clear green supernatant was measured spectrophotometrically at 695 nm against an appropriate blank. TAC was calculated using the molar extinction coefficient (ε) of (3.4 ± 0.1) × $10^3$ $M^{-1}$ $cm^{-1}$ for the phosphomolybdenum complex and expressed as micromoles per milligram of protein (μmol/mg protein), representing the concentration of reducing species equivalents per liter.

#### *2.5.5. Membrane-bound activities*

Total ATPase activity in kidney and serum samples was determined by measuring inorganic phosphate (Pi) released from the hydrolysis of ATP, as described by Tsakiris and Deliconstantinos.[57] The reaction mixture contained 40 mM Tris-HCl buffer (pH 7.4), 5 mM $MgCl_2$, 80 mM NaCl, 20 mM KCl, and 0.1 mL of sample, adjusted to a final volume of 1.0 mL with distilled water. The reaction was initiated by adding disodium ATP to a final concentration of 3 mM, and the mixture was incubated at room temperature for 30 min. Enzymatic activity was terminated by adding 0.5 mL of 5% SDS. Liberated Pi was then quantified using the molybdenum blue method.[58] The reaction volume was adjusted to 2.4 mL with distilled water, followed by the addition of 0.8 mL of 3 N $H_2SO_4$ and 0.4 mL of 2.5% (w/v) ammonium molybdate in 3 N $H_2SO_4$. Subsequently, 0.4 mL of reducing reagent (containing 20 mg/mL each of hydrazine sulfate and ascorbic acid in 0.1 N $H_2SO_4$) was added. After incubation for 30 min to allow color development, absorbance was measured at 820 nm against a reagent blank. ATPase activity was expressed as U/mg of protein, where one unit represents the amount of enzyme that liberates one micromole of Pi per minute under the assay conditions.

Furthermore, $Ca^{2+}$/$Mg^{2+}$-ATPase activity in kidney and serum samples was assayed using a method adapted from Hanahan and Ekholm[59], following the same principle of Pi liberation measurement as the total ATPase assay but with modifications in reaction conditions to specifically measure $Ca^{2+}$/$Mg^{2+}$-dependent activity. The assay was performed in a specially formulated reaction cocktail containing 80 mM Tris-HCl buffer (pH 7.6), 3.6 mM $MgCl_2$, 2.5 mM disodium ATP, 80 mM NaCl, 33 mM KCl, and 0.50 mM $CaCl_2$. A 0.1 mL sample aliquot was added to 0.5 mL of this cocktail mixture. The reaction was incubated for 30 min at 44 °C to optimize enzymatic activity, then terminated by adding 0.3 mL of 5% SDS. The quantification of liberated Pi was carried out using the molybdenum blue method described by Katewa and Katyare[58], as detailed in the previous section for total ATPase measurement. This method involves the formation of a phosphomolybdate complex that is reduced to a blue-colored compound, with absorbance measured spectrophotometrically. $Ca^{2+}$/$Mg^{2+}$-ATPase activity was calculated based on the amount of Pi liberated per minute per milligram of protein under these specific cation conditions. One unit of enzyme activity was defined as the amount that hydrolyzes ATP to release one micromole of inorganic phosphate per minute under the standard assay conditions. Results were expressed as U/mg of protein.

#### *2.5.6. Inflammatory markers*

Nitric oxide levels were quantified in kidney homogenate by using the Griess reaction, which measures the stable end products of NO metabolism, nitrite ($NO_2^-$) and nitrate ($NO_3^-$), as described by Green *et al.*[60] In biological systems, •NO is synthesized by NO synthase via a five-electron oxidation of L-arginine to citrulline. Due to its short half-life, •NO is rapidly oxidized to $NO_2^-$ and $NO_3^-$, which serve as indirect markers of NO production.

To accurately assess total NO levels, $NO_3^-$ was first reduced to $NO_2^-$ using enzymatic reduction with nitrate reductase or chemical reduction using cadmium/vanadium-based methods. The Griess reaction involves a two-step diazotization process in which $NO_2^-$ reacts with sulfanilamide in an acidic medium to form a diazonium salt, which then couples with N-1-naphthylethylenediamine dihydrochloride (NEDD) to yield a stable purple/magenta azo chromophore.

Briefly, 100 µL of sample was mixed with 100 µL of 1% (w/v) sulfanilamide solution (prepared in 5% phosphoric acid) and incubated in the dark for 15 min at room temperature. Then, 1 mL of 0.1% (w/v) NEDD solution was added, mixed thoroughly, and incubated for an additional 10 min in the dark. The absorbance of the resulting azo dye was measured at 520 nm within 15 min after the addition of NEDD, using a spectrophotometer and a cuvette with a 1 cm path length. NO concentration was determined from a standard curve prepared with sodium nitrite (0–100 nM), and results were expressed as nanomoles per gram of tissue (nmol/g tissue).[61,62] The sensitivity and specificity of the assay were maintained by including appropriate blanks to account for background absorbance and potential interference.

Myeloperoxidase activity was determined spectrophotometrically based on the enzyme's catalytic oxidation of guaiacol in the presence of hydrogen peroxide, as described by Hasmann *et al.*[63] MPO, a pro-inflammatory enzyme abundant in neutrophil azurophilic granules, catalyzes the formation of a brown tetraguaiacol product which absorbs strongly at 470 nm. For the assay, 0.1 mL of sample was combined with 4.4 mL of substrate solution (containing 100 mM guaiacol and 0.017% $H_2O_2$ in 50 mM potassium phosphate buffer, pH 7.0) in a cuvette with a 1 cm path length. The reaction kinetics were monitored by measuring the increase in absorbance at 470 nm every 30 s for 3 min. MPO activity was calculated using the molar extinction coefficient of $5.58 \times 10^3$ $M^{-1}$ $cm^{-1}$ for oxidized guaiacol, with one unit of activity defined as the amount of enzyme required to oxidize one micromole of guaiacol per minute under the specified conditions. Results were expressed as units per gram of protein (U/g protein $\times 10^{-3}$).

Additionally, IFN-γ and IL-1β levels in kidney tissue were determined using ElabScience rat ELISA kits, according to the manufacturer's instructions. Briefly, 100 µL of standards or samples were added to the antibody-coated wells and incubated for 90 min at 37 °C. After discarding the liquid, 100 µL of biotinylated detection antibody working solution was added to each well and incubated for 60 min at 37 °C. The wells were then aspirated and washed three times to remove unbound materials, after which 100 µL of horseradish peroxidase-conjugate working solution was added and the plate was incubated for 30 min at 37 °C. Following incubation, the wells were washed five times, and 90 µL of 3,3',5,5'-tetramethylbenzidine substrate reagent was added, with further incubation for 15 min at 37 °C to allow color development. The enzymatic reaction was stopped by adding 50 µL of stop solution, and the absorbance was immediately measured at 450 nm using a Biobase EL-10A microplate reader (Biobase, China). Results were expressed as pg/mL.

### 2.6. Statistical analysis

Data analysis was performed using Statistical Package for Social Sciences (SPSS) version 23.0 (IBM, USA), and graphs were plotted using GraphPad Prism version 10.0 (GraphPad, USA). The statistical significance of differences between groups was analyzed using one-way analysis of variance (ANOVA), followed by Tukey's post hoc test. The significance level was set at $p < 0.05$ and presented as mean ± standard error of the mean (SEM).

## 3. Results

Table 2 shows the effect of chrysin on PFOA-induced kidney dysfunction in tissue creatinine, LDH, and electrolytes of male Wistar rats. The findings show that 5 mg/kg of PFOA increased kidney creatinine significantly ($p < 0.05$) by 25.74% compared to control; pre-treatment with chrysin reduced this PFOA-induced increase by 22.57% at 25 mg/kg and by 20.21% at 50 mg/kg compared to the PFOA-only group. Tissue LDH activity increased significantly ($p < 0.05$) by 41.29% with PFOA, and chrysin strongly suppressed this increase, reducing LDH by 71.60% at 25 mg/kg and by 70.66% at 50 mg/kg compared to the PFOA-only group.

Kidney sodium level increased significantly ($p < 0.05$) by 19.80% compared to control, and the PFOA-induced sodium rise was attenuated by chrysin by 16.53% at 25 mg/kg and by 14.97% at 50 mg/kg compared to the PFOA-only group. Kidney potassium level decreased significantly ($p < 0.05$) by 50.54% compared to control; both chrysin doses restored tissue potassium compared to the PFOA-only group, with increases of 120.94% at 25 mg/kg and 91.34% at 50 mg/kg. Kidney calcium level increased by

36.67% compared to control and was reduced by chrysin pre-treatment, with decreases of 30.79% at 25 mg/kg and 27.46% at 50 mg/kg compared to the PFOA-only group. Kidney magnesium level decreased by 18.64% with PFOA ($p < 0.05$) and was increased by chrysin pre-treatment, with increases of 40.28% at 25 mg/kg and 31.25% at 50 mg/kg compared to the PFOA-only group. Importantly, the chrysin-only group and both chrysin pre-treatment groups (25 and 50 mg/kg) were not significantly different from the control group for all kidney markers ($p > 0.05$).

Table 3 shows the effect of chrysin on PFOA-induced changes in serum creatinine and electrolytes of male Wistar rats. The findings reveal that treatment with 5 mg/kg of PFOA increased serum creatinine by 22.58% compared to normal control ($p < 0.05$); chrysin pre-treatment lowered this increase by 15.79% at 25 mg/kg and by 21.05% at 50 mg/kg compared to the PFOA-only group. PFOA decreased serum sodium level by 18.28% compared to control; chrysin restored serum sodium with increases of 28.78% at 25 mg/kg and 17.62% at 50 mg/kg compared to the PFOA-only group. Serum potassium level increased by 46.08% after PFOA exposure ($p < 0.05$); chrysin produced a non-significant decrease of 23.49% at 25 mg/kg compared to the PFOA-only group ($p > 0.05$) and a significant decrease of 42.06% at 50 mg/kg compared to the PFOA-only group ($p < 0.05$). Serum calcium level decreased by 22.26% with PFOA and was increased by chrysin pre-treatment, with increases of 62.82% at 25 mg/kg and 30.97% at 50 mg/kg compared to the PFOA-only group. Serum magnesium level showed no significant differences across groups ($p > 0.05$). Serum creatinine and electrolyte levels in the chrysin-only group were comparable to control values, with no significant difference observed. Overall, chrysin at both doses largely reversed the PFOA-induced serum abnormalities, with the 50 mg/kg dose producing the clearest normalization of potassium and creatinine.

### 3.1. Chrysin attenuates PFOA-induced renal oxidative stress

Exposure to PFOA resulted in a significant elevation ($p < 0.05$) of kidney MDA levels, which were 106.56% higher than those of the control group (Figure 2A). Pre-treatment with chrysin effectively reduced this PFOA-induced

**Table 2. Effect of chrysin on PFOA-induced renal dysfunction in male Wistar rats**

| Groups (treatments) | Creatinine (μmol/g) | LDH (U/g protein) | Na (mEq/L) | K (mmol/L) | Ca (mg/dL) | Mg (mg/dL) |
|---|---|---|---|---|---|---|
| Control (20% DMSO) | 3.03 ± 0.01$^{a}$ | 47.23 ±1.12$^{b}$ | 170.86 ± 1.30$^{a}$ | 5.60 ± 0.61$^{b}$ | 22.96 ± 1.39$^{a}$ | 1.77 ± 0.17$^{b}$ |
| 5 mg/kg PFOA-only | 3.81 ± 0.01$^{b}$ | 66.73 ± 4.03$^{c}$ | 204.69 ± 2.66$^{b}$ | 2.77 ± 0.20$^{a}$ | 36.67 ± 1.53$^{b}$ | 1.44 ± 0.06$^{a}$ |
| 25 mg/kg chrysin + 5 mg/kg PFOA | 2.95 ± 0.04$^{a}$ | 18.95 ± 1.16$^{a}$ | 170.86 ± 9.40$^{a}$ | 6.12 ± 0.46$^{b}$ | 25.38 ± 2.01$^{a}$ | 2.02 ± 0.03$^{b}$ |
| 50 mg/kg chrysin + 5 mg/kg PFOA | 3.04 ± 0.16$^{a}$ | 19.58 ± 0.68$^{a}$ | 174.04 ± 3.57$^{a}$ | 5.30 ± 0.31$^{b}$ | 26.60 ± 1.35$^{a}$ | 1.89 ± 0.04$^{b}$ |
| 50 mg/kg chrysin-only | 3.04 ± 0.08$^{a}$ | 18.16 ± 0.23$^{a}$ | 182.39 ± 4.84$^{a}$ | 4.90 ± 0.20$^{b}$ | 27.97 ± 2.63$^{a}$ | 1.94 ± 0.06$^{b}$ |

Notes: Data are presented as mean ± standard error of the mean ($n = 5$) and analyzed using one-way ANOVA followed by Tukey's post hoc test. Means within a column not sharing a common superscript letter ($^{a}$, $^{b}$, and $^{c}$) differ significantly ($p < 0.05$).
Abbreviations: DMSO: Dimethyl sulfoxide; LDH: Lactate dehydrogenase; PFOA: Pentadecafluorooctanoic acid.

**Table 3. Effect of chrysin on PFOA-induced renal dysfunction in male Wistar rats**

| Groups (treatments) | Creatinine (μmol/L) | Na (mEq/L) | K (mmol/L) | Ca (mg/dL) | Mg (mg/dL) |
|---|---|---|---|---|---|
| Control (20% DMSO) | 0.31 ± 0.01$^{a}$ | 176.83 ± 2.97$^{b}$ | 3.06 ± 0.20$^{ab}$ | 26.33 ± 2.22$^{b}$ | 1.82 ± 0.06 |
| 5 mg/kg PFOA-only | 0.38 ± 0.00$^{b}$ | 144.50 ± 4.33$^{a}$ | 4.47 ± 0.55$^{b}$ | 20.47 ± 0.46$^{a}$ | 2.03 ± 0.07 |
| 25 mg/kg chrysin + 5 mg/kg PFOA | 0.32 ± 0.01$^{a}$ | 186.09 ± 9.93$^{b}$ | 3.42 ± 0.36$^{ab}$ | 33.33 ± 0.46$^{c}$ | 1.76 ± 0.04 |
| 50 mg/kg chrysin + 5 mg/kg PFOA | 0.30 ± 0.11$^{a}$ | 169.96 ± 3.94$^{b}$ | 2.59 ± 0.30$^{a}$ | 26.81 ± 1.02$^{b}$ | 1.91 ± 0.09 |
| 50 mg/kg chrysin-only | 0.28 ± 0.02$^{a}$ | 181.17 ± 6.02$^{b}$ | 2.87 ± 0.24$^{a}$ | 27.18 ± 1.20$^{b}$ | 1.81 ± 0.14 |

Notes: Data are presented as mean ± standard error of the mean ($n = 5$) and analyzed using one-way ANOVA followed by Tukey's post hoc test. Means within a column not sharing a common superscript letter ($^{a}$, $^{b}$, and $^{c}$) differ significantly ($p < 0.05$).
Abbreviations: DMSO: Dimethyl sulfoxide; PFOA: Pentadecafluorooctanoic acid.

increase. The 25 mg/kg chrysin dose reduced MDA levels by 39.95% compared to the PFOA-only group, and MDA levels in this group showed no significant difference ($p > 0.05$) from the control group. In contrast, the 50 mg/kg chrysin dose reduced MDA by 35.98% compared to the PFOA group; however, MDA levels in this group remained 32.24% higher than the control group—a statistically significant difference ($p < 0.05$). The 50 mg/kg chrysin-only group showed no significant difference ($p > 0.05$) from the control group.

Moreover, PFOA administration caused a significant ($p < 0.05$) depletion of renal reduced GSH by 21.55% compared to the control group (Figure 2B). Chrysin pre-treatment at 25 mg/kg and 50 mg/kg attenuated this depletion, elevating GSH levels by 64.99% and 62.69%, respectively, compared to the PFOA group. Furthermore, these pre-treatment groups showed GSH levels that were 29.44% and 27.64% higher than the control group ($p < 0.05$). The Chrysin-only group showed a 16.14% decrease compared to the control ($p > 0.05$) and no significant difference from the PFOA-only group.

### 3.2. Chrysin normalizes renal antioxidant enzyme activities and total antioxidant capacity

The activity of SOD declined significantly ($p < 0.05$) in the PFOA group by 44.93% compared to the control (Figure 3A). Chrysin pre-treatment at 25 mg/kg and 50 mg/kg elevated SOD activity by 81.57% and 67.14%, respectively, compared to the PFOA-only group, with both not significantly different ($p > 0.05$) from the control group. The chrysin-only group showed a significant increase of 27.49% ($p < 0.05$) compared to the control.

Renal CAT activity decreased significantly ($p < 0.05$) by 54.63% in the PFOA group compared to the normal control group (Figure 3B). Both chrysin doses enhanced CAT activity, with the 25 mg/kg and 50 mg/kg pre-treatment

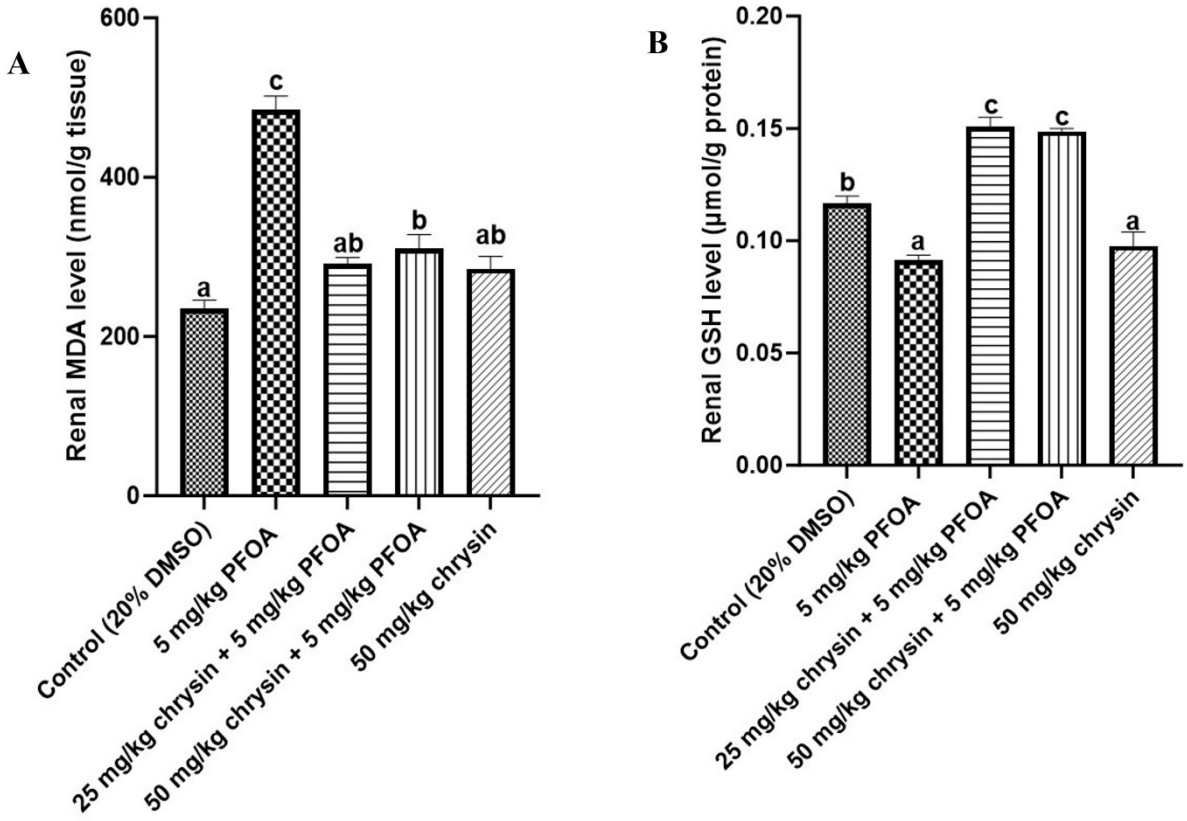


**Figure 2.** Nephroprotective effect of chrysin on PFOA-induced renal oxidative stress markers in male Wistar rats: (A) renal MDA and (B) renal GSH. Data are expressed as mean ± standard error of the mean ($n = 5$). All groups were compared using Tukey's post hoc test. Bars with different letters (a–c) differ significantly from one another ($p < 0.05$), whereas bars sharing the same letter or at least one letter do not differ significantly.
Abbreviations: DMSO: Dimethyl sulfoxide; GSH: Glutathione; MDA: Malondialdehyde; PFOA: Pentadecafluorooctanoic acid.

doses showing significant increases ($p < 0.05$) of 72.62% and 56.45%, respectively, compared to the PFOA-only group. However, the activity in both pre-treatment groups remained significantly lower than that of the control group ($p < 0.05$), with the 25 mg/kg and 50 mg/kg doses showing a decrease of 21.68% and 29.02%, respectively. The chrysin-only group showed no significant difference ($p > 0.05$) from the control group.

Kidney GPx activity was significantly suppressed ($p < 0.05$) by 66.52% in the PFOA group compared to the control group (Figure 3C). Chrysin pre-treatment reversed this suppression, increasing activity by 123.22% (25 mg/kg) and 110.42% (50 mg/kg) compared to the PFOA-only group. The chrysin-only group also significantly increased GPx activity by 192.78% compared to the PFOA-only group. However, the activity in the 25 mg/kg and 50 mg/kg pre-treatment groups remained 25.27% and 29.55% lower, respectively, than the control group ($p < 0.05$). The Chrysin-only group showed no significant difference ($p > 0.05$) from the control.

Renal GST activity was markedly reduced ($p < 0.05$) by 81.25% in the PFOA group (Figure 3D). Chrysin pre-treatments restored GST activity by 275.77% (25 mg/kg) and 303.73% (50 mg/kg), achieving levels not significantly different ($p > 0.05$) from the control. The chrysin-only group showed a significant increase of 248.20% ($p < 0.05$) compared to the control and was 394.07% and 359.85% higher than the 25 mg/kg and 50 mg/kg pre-treatment groups, respectively.

The PFOA group exhibited a significant reduction ($p < 0.05$) in kidney TAC by 17.44% relative to the control (Figure 3E). Both chrysin doses restored TAC levels. The 25 mg/kg pre-treatment increased TAC by 61.34%, and the 50 mg/kg pre-treatment increased it by 46.72% compared to the PFOA-only group; the 25 mg/kg dose showed a slightly greater increase, though the difference between the two pre-treatment doses was not statistically significant ($p > 0.05$). When compared to the control group, the 25 mg/kg pre-treatment group showed a significant increase of 33.21% ($p < 0.05$), while the 50 mg/kg pre-treatment group showed an increase of 21.13% that was not statistically significant ($p > 0.05$). The chrysin-only group showed a significant increase of 63.42% ($p < 0.05$) compared to the control. Furthermore, the chrysin-only group also showed a significant increase of 97.94% compared to the PFOA-only group, and significant increases of 22.8% and 34.91% compared to the 25 mg/kg and 50 mg/kg Chrysin pre-treatment groups, respectively.

### 3.3. Chrysin pre-treatment rescues rats from membrane-bound marker imbalances

The findings reveal that PFOA administration (5 mg/kg) significantly suppressed ($p < 0.05$) total ATPase activity by 59.97% in renal tissue compared to the control group. Chrysin pre-treatment (25 and 50 mg/kg) attenuated this suppression, with both doses significantly ($p < 0.05$) restoring ATPase activity by 112.36% and 93.02%, respectively, compared to the PFOA-only group. There was no significant difference ($p > 0.05$) between the two chrysin pre-treatment doses, although the 25 mg/kg dose showed a slightly greater increase. Notably, the 50 mg/kg chrysin-only group exhibited activity levels comparable to the control (Figure 4A).

Serum total ATPase activity was markedly reduced in the PFOA group by 71.97% compared to the control group ($p < 0.05$). In contrast, chrysin pre-treatment (25 and 50 mg/kg) and the 50 mg/kg chrysin-only group significantly elevated serum ATPase activity by 516.76%, 238.06%, and 275.40%, respectively, with the 25 mg/kg chrysin pre-treatment showing the greatest increase compared to the PFOA-only group ($p < 0.05$). Additionally, the 25 mg/kg chrysin pre-treatment group showed a significant increase of 72.88% compared to the control group, while the 50 mg/kg chrysin pre-treatment and chrysin-only groups showed no significant difference from the control group (Figure 4B).

Renal $Ca^{2+}/Mg^{2+}$-ATPase activity was significantly impaired by PFOA (57.57%) compared to normal control animals ($p < 0.05$). Chrysin pre-treatment (25 and 50 mg/kg) and the 50 mg/kg chrysin-only group reversed this deficit, restoring activity to near-control levels ($p < 0.05$). Moreover, no significant difference was observed between the 25 and 50 mg/kg chrysin pre-treatment groups; however, these two doses showed significant increases of 129.89% and 114.72%, respectively, compared to the PFOA-only group (Figure 4C). PFOA exposure caused a significant reduction in serum $Ca^{2+}/Mg^{2+}$-ATPase activity by 52.97% compared to the normal control group ($p < 0.05$). Furthermore, chrysin pre-treatment (25 and 50 mg/kg) demonstrated a dose-dependent therapeutic response, with the 25 mg/kg chrysin pre-treatment partially restoring ATPase activity by 248.44% compared to the PFOA-only group, although it remained significantly lower than the control group (41.93% decrease, $p < 0.05$). However, the 50 mg/kg chrysin pre-treatment fully restored enzyme activity, showing a 521.10% increase compared to the PFOA-only group and no significant difference from the control group ($p > 0.05$), indicating superior efficacy compared to the 25

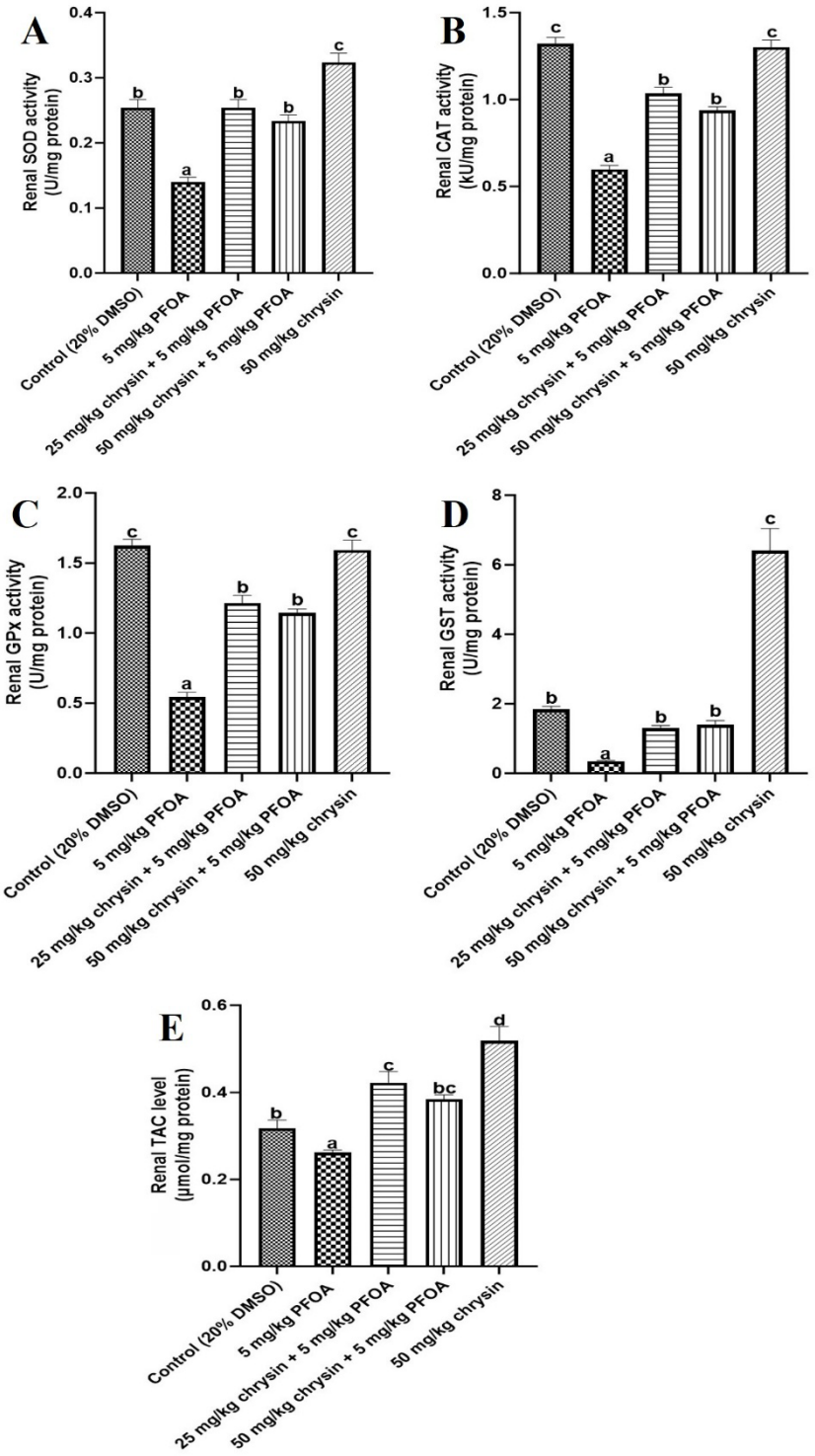


**Figure 3.** Nephroprotective effect of chrysin on PFOA-induced renal antioxidant enzymes in male Wistar rats: (A) renal SOD, (B) renal CAT, (C) renal GPx, (D) renal GST, and (E) renal TAC. Data are expressed as mean ± standard error of the mean ($n = 5$). All groups were compared using Tukey's post hoc test. Bars with different letters (a–c) differ significantly from one another ($p < 0.05$), whereas bars sharing the same letter or at least one letter do not differ significantly.

Abbreviations: CAT: Catalase; DMSO: Dimethyl sulfoxide; GPx: Glutathione peroxidase; GST: Glutathione S-transferase; PFOA: Pentadecafluorooctanoic acid; SOD: Superoxide dismutase; TAC: Total antioxidant capacity.

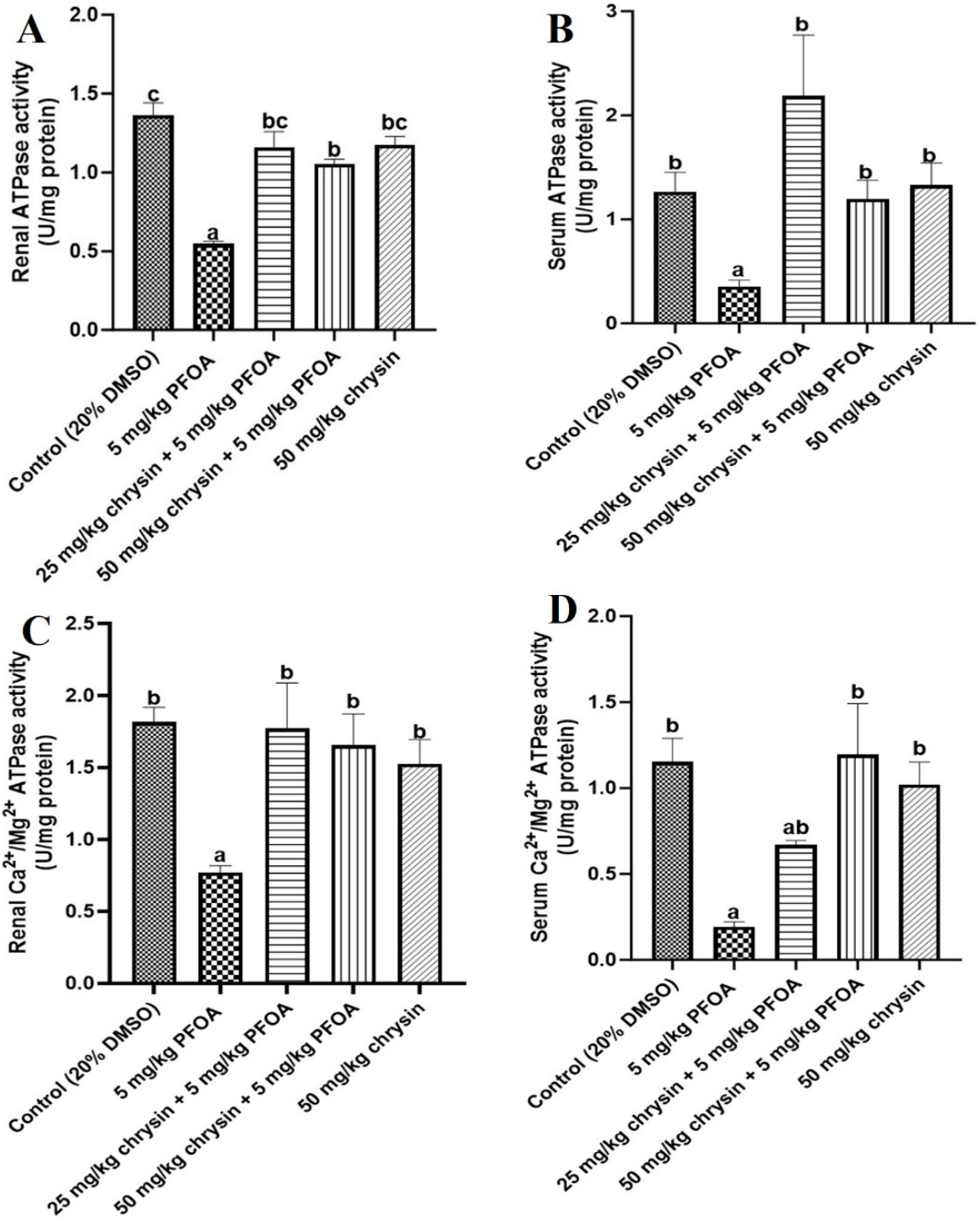


**Figure 4.** Nephroprotective effect of chrysin on PFOA-induced alterations in serum and renal membrane-bound marker activities in male Wistar rats: (A) renal ATPase activity, (B) serum ATPase activity, (C) renal $Ca^{2+}/Mg^{2+}$ ATPase activity, and (D) serum $Ca^{2+}/Mg^{2+}$ ATPase activity. Data are expressed as mean ± standard error of the mean ($n = 5$). All groups were compared using Tukey's post hoc test. Bars with different letters (a–c) differ significantly from one another ($p < 0.05$), whereas bars sharing the same letter or at least one letter do not differ significantly.
Abbreviations: DMSO: Dimethyl sulfoxide; PFOA: Pentadecafluorooctanoic acid.

mg/kg regimen ($p < 0.05$). In addition, the chrysin-only group showed no significant difference from the normal control group (Figure 4D).

### 3.4. Chrysin pre-treatment attenuates PFOA-induced inflammatory and pro-inflammatory cytokines

Exposure to PFOA significantly suppressed kidney NO levels by 44.21% compared to the control group ($p < 0.05$). Chrysin pre-treatment restored NO concentrations at both 25 and 50 mg/kg doses by 121.86% and 106.14% when compared to the PFOA-only group. No significant difference was observed between chrysin pre-treatment doses or between either dose and the normal control group. Additionally, no significant difference was observed between the 50 mg/kg chrysin-only group and the normal control group (Figure 5A).

Furthermore, renal MPO activity increased significantly ($p < 0.05$) in PFOA-exposed rats by 88.45% compared to the control group. Chrysin pre-treatment reduced renal MPO activity, with the 25 mg/kg dose showing a more marked reduction by 74.82%, while the 50 mg/kg dose decreased renal MPO activity by 62.22% compared to the PFOA-only group. The 25 mg/kg dose chrysin pre-treatment group also showed a significant decrease of 52.55% compared to the control group, while the 50 mg/kg chrysin pre-treatment showed levels comparable to the control group. No significant difference was observed between the chrysin-only group and the normal control group (Figure 5B).

Systemic inflammation was evident in the PFOA group, as indicated by elevated serum MPO activity (172.49%) relative to the control group ($p < 0.05$). Chrysin pre-treatment reduced serum MPO activity, with the 50 mg/kg dose yielding a greater ameliorative effect by 67.80% compared to the PFOA-only group. The 25 mg/kg chrysin pre-treatment showed a 50.95% decrease compared to the PFOA-only group. No significant difference was observed between the chrysin pre-treatment groups or between either group and the control group ($p > 0.05$). In addition, no significant difference was observed between the 50 mg/kg chrysin-only group and the control group (Figure 5C).

Moreover, PFOA administration (5 mg/kg) significantly elevated IFN-γ levels in renal tissue compared to the control group by 33.28% ($p < 0.05$). The 25 and 50 mg/kg chrysin pre-treatment reduced IFN-γ concentrations in a dose-dependent manner, with both doses demonstrating a stronger attenuating effect by 25.27% and 32.72%, respectively, compared to the PFOA-only group. Chrysin pre-treatment groups showed no significant difference between them, or when compared to the chrysin-only group or the normal control group. No significant difference was observed between the chrysin-only group and the control group (Figure 5D).

Renal IL-1β levels increased significantly in the PFOA-exposed group by 55.27% compared to the normal control group ($p < 0.05$). Chrysin pre-treatment diminished IL-1β concentrations, with both doses (25 and 50 mg/kg) showing pronounced reduction by 40.95% and 36.47%, respectively, compared to the PFOA-only group. No significant difference was observed between the chrysin pre-treatment groups compared to the normal control or the chrysin-only group. Additionally, no significant difference was observed between the chrysin-only group and the control group (Figure 5E).

## 4. Discussion

The present study provides compelling evidence that chrysin, a natural flavonoid, confers significant nephroprotection against PFOA-induced renal injury in male Wistar rats. The multifaceted toxicological profile of PFOA, a pervasive environmental pollutant with documented nephrotoxic effects, includes the induction of oxidative stress, inflammation, and disruption of cellular energy transport systems.[10,64] These findings are consistent with previous reports demonstrating that chrysin exerts nephroprotective effects through multiple pharmacodynamic mechanisms, including attenuation of oxidative stress, modulation of inflammatory responses, preservation of mitochondrial function, and stabilization of cellular membranes in experimental models of kidney injury.[16,65] Despite these promising pharmacological properties, the clinical translation of chrysin remains limited because of its poor aqueous solubility, low oral bioavailability, and extensive first-pass metabolism through glucuronidation and sulfation.[66,67] Nevertheless, available evidence indicates that chrysin is generally well tolerated at commonly investigated doses, although comprehensive human safety data remain limited. Potential interactions with drugs metabolized by cytochrome P450 enzymes and phase II conjugating enzymes have also been suggested, warranting caution during concurrent administration until further clinical studies establish its long-term safety, efficacy, and pharmacokinetic profile in humans.[66,68]

Exposure to PFOA significantly elevated serum and renal creatinine levels (Table 2), suggesting impaired glomerular filtration and tubular dysfunction, consistent with its role in disrupting renal hemodynamics and ion transport.[10,69,70] The increase in serum creatinine concentration specifically reflects reduced glomerular filtration rate, a primary indicator of renal functional impairment following toxicant exposure.[71] Chrysin pre-

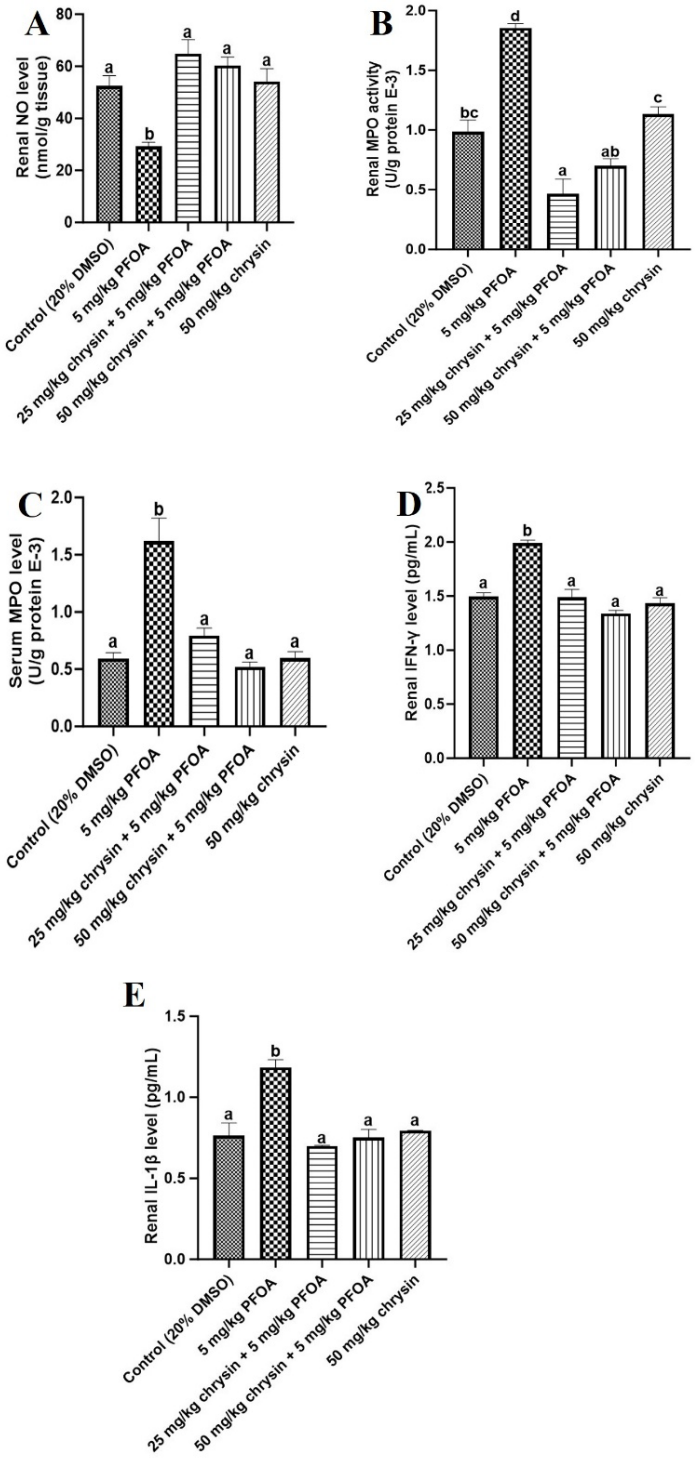


**Figure 5.** Nephroprotective effect of chrysin on PFOA-induced alterations in serum and renal inflammatory markers and pro-inflammatory cytokines in male Wistar rats: (A) NO, (B) renal MPO activity, (C) serum MPO level, (D) kidney IFN-γ level, and (E) renal IL-1β level. Data are expressed as mean ± standard error of the mean ($n = 5$). All groups were compared using Tukey's post hoc test. Bars with different letters (a–c) differ significantly from one another ($p < 0.05$), whereas bars sharing the same letter or at least one letter do not differ significantly.

Abbreviations: DMSO: Dimethyl sulfoxide; IFN: Interferon; IL: Interleukin; MPO: Myeloperoxidase; NO: Nitric oxide; PFOA: Pentadecafluorooctanoic acid.

treatment normalized creatinine levels, aligning with its ability to preserve glomerular integrity, as previously observed in cisplatin- and methotrexate-induced nephrotoxicity.[3,8,72,73] This normalization effect suggests that chrysin helps maintain filtration barrier function and prevents the decline in glomerular filtration rate typically associated with PFOA-induced nephrotoxicity.

Similarly, LDH activity, a sensitive marker of cellular injury and necrosis, was markedly elevated in the kidney following PFOA exposure (Table 2), indicating substantial cellular membrane damage and leakage of intracellular enzymes.[74] This elevation reflects PFOA-induced cytotoxic effects on renal tubular cells, including mitochondrial dysfunction and plasma membrane disruption.[75,76] The significant reduction in LDH levels following chrysin pre-treatment demonstrates its membrane-stabilizing properties and ability to mitigate necrotic damage to renal cells, consistent with earlier reports of chrysin's cytoprotective effects in various models of organ toxicity.[2,77] Interestingly, renal LDH activity in the chrysin-treated groups declined to values lower than those of the control group. This observation may reflect not only attenuation of cellular injury but also reduced metabolic stress and improved mitochondrial oxidative metabolism, thereby decreasing the reliance on anaerobic glycolysis, in which LDH plays a pivotal role.[78,79] Consequently, the reduced tissue LDH activity may indicate enhanced metabolic efficiency and restoration of cellular homeostasis following chrysin treatment rather than an adverse suppression of physiological enzyme function, consistent with the metabolic normalization observed following antioxidant interventions in experimental models of tissue injury.[2,65]

Electrolyte imbalances observed in both serum and renal tissue (Tables 2 and 3) reflect PFOA-induced disruption of ATP-dependent ion pumps, particularly $Ca^{2+}$/$Mg^{2+}$-ATPase and total ATPase.[80] The perturbation of potassium homeostasis, manifested as hyperkalemia, suggests impaired renal tubular secretion mechanisms, potentially due to PFOA-mediated inhibition of ion channels and transporters in the distal convoluted tubule of the nephron.[81,82] Similarly, alterations in calcium and magnesium levels indicate disrupted reabsorption processes in the thick ascending limb and distal convoluted tubule.[83,84] Chrysin restored these electrolytes to near-normal levels, indicating preservation of tubular transport function through maintenance of ATPase activity and cellular energy metabolism.[2,8,85] This effect may be attributed to chrysin's ability to maintain cellular integrity and ATPase functionality, thereby supporting active ion transport processes critical for renal homeostasis.[86]

Moreover, PFOA-induced oxidative stress was evident in elevated MDA levels (Figure 2A), indicating excessive lipid peroxidation and reactive oxygen species (ROS) generation.[14] PFOA bioaccumulation in renal tissues disrupts mitochondrial electron transport chains through its protein-binding properties, leading to superoxide anion production and subsequent oxidative damage to cellular lipids, proteins, and DNA.[10,12,87] The concomitant depletion of reduced GSH (Figure 2B) further exacerbates oxidative injury, as GSH serves as a critical intracellular antioxidant that neutralizes ROS and facilitates detoxification of electrophilic compounds.[88] The decreased activities of antioxidant enzymes, including SOD, CAT, GPx, and GST (Figure 3A–3D) represent additional mechanisms through which PFOA compromises the renal antioxidant defense system.

Chrysin pre-treatment reduced MDA levels and restored GSH concentrations in a dose-dependent manner (Figure 2A and 2B), highlighting its potent antioxidant activity through multiple mechanisms, including direct scavenging of free radicals due to the phenolic hydroxyl groups in its chemical structure. The restoration of endogenous antioxidant defenses observed following chrysin pre-treatment may be associated with activation of the Nrf2 signaling pathway. Previous studies have demonstrated that chrysin enhances Nrf2 nuclear translocation and promotes the expression of downstream cytoprotective genes, including those encoding HO-1, NAD(P)H quinone oxidoreductase-1, GSH-related enzymes, and other antioxidant proteins in models of oxidative tissue injury. The observed restoration of antioxidant enzymes and reduced lipid peroxidation is consistent with the antioxidant mechanisms previously reported for chrysin.[72,89,90] The Nrf2 pathway upregulation leads to increased transcription of antioxidant response element-regulated genes, including those encoding

glutamate-cysteine ligase, the rate-limiting enzyme in GSH synthesis.[89,91] Additionally, chrysin restored the activities of key antioxidant enzymes, including SOD (Figure 3A), which catalyzes the dismutation of superoxide radicals to hydrogen peroxide; CAT and GPx (Figure 3B and 3C), which detoxify hydrogen peroxide; and GST (Figure 3D), which facilitates the conjugation of GSH to electrophilic toxins for enhanced excretion.[3,92] The recovery of these enzymes underscores chrysin's role in reinforcing the renal antioxidant defense system through both direct free radical scavenging and enhancement of endogenous antioxidant capacity.

Total antioxidant capacity was significantly depleted in PFOA-exposed rats (Figure 3E) but was restored by chrysin pre-treatment. TAC represents the cumulative ability of both enzymatic and non-enzymatic antioxidants to counteract oxidative stress[93], and its depletion reflects the overall compromise of antioxidant defenses following PFOA exposure. Chrysin's ability to elevate TAC further confirms its comprehensive antioxidant action, which is crucial for mitigating PFOA-induced redox imbalance and preventing oxidative damage to cellular components.

Additionally, PFOA exposure significantly impaired the activities of total ATPase and $Ca^{2+}/Mg^{2+}$-ATPase in both renal tissue and serum (Figure 4A–4D). These enzymes are critical for maintaining electrochemical gradients across membranes, regulating ion transport, and supporting cellular energy metabolism.[94,95] Total ATPase includes $Na^+/K^+$-ATPase, which is essential for sodium and potassium homeostasis and maintenance of the membrane potential, while $Ca^{2+}/Mg^{2+}$-ATPase regulates intracellular calcium levels and prevents calcium-mediated cytotoxicity.[96,97] PFOA-induced inhibition of these pumps likely results from multiple mechanisms, including lipid peroxidation-mediated damage to membrane integrity, direct binding to enzyme subunits, or ROS-induced protein oxidation.[10,12]

Chrysin pre-treatment notably restored ATPase activities, with the 50 mg/kg dose exhibiting superior efficacy (Figure 4). This recovery can be attributed to chrysin's ability to reduce lipid peroxidation, thereby preserving membrane fluidity and integrity necessary for proper ATPase function.[2,72] Additionally, by enhancing antioxidant defenses and reducing oxidative stress, chrysin minimizes oxidative modifications of ATPase proteins, ensuring their functional competence and preventing enzyme inactivation.[89,91] The restoration of $Ca^{2+}/Mg^{2+}$-ATPase is particularly important for preventing calcium overload, which can trigger apoptosis, mitochondrial dysfunction, and activation of calcium-dependent proteases.[8,85,98,99] These findings align with previous studies where chrysin ameliorated ATPase dysfunction in various models of cytotoxicity.[2,72,100,101]

In addition, PFOA exposure triggered a robust inflammatory response, characterized by elevated levels of pro-inflammatory cytokines and markers. NO levels were suppressed in PFOA-exposed rats (Figure 5A), likely due to oxidative inactivation of NO or reduced endothelial NO synthase activity.[102] NO is crucial for renal vasodilation, blood flow regulation, and maintenance of glomerular filtration rate, in addition to its antioxidant properties through reaction with superoxide radicals.[103,104] Chrysin restored NO levels, possibly by reducing oxidative stress and preventing the reaction between NO and superoxide to form peroxynitrite, as well as by enhancing endothelial NO synthase expression. This restoration of NO bioavailability contributes to improved renal hemodynamics and helps mitigate ischemic injury in the kidney.[90,105–107]

Myeloperoxidase activity, a marker of neutrophil infiltration and oxidative burst, was increased in both serum and renal tissue in the PFOA-treated group (Figure 5B and 5C).[108,109] Furthermore, PFOA exposure increased the levels of IFN-γ and IL-1β in renal tissue (Figure 5D and 5E).[10,12,110,111] PFOA activates innate immune responses through pattern recognition receptors and promotes the release of damage-associated molecular patterns from damaged cells, which initiate inflammatory cascades.[112,113] Specifically, PFOA has been shown to activate the NLRP3 inflammasome, leading to caspase-1–mediated cleavage and secretion of IL-1β.[12,109,114] IFN-γ, which is primarily released by activated T cells and natural killer cells, exacerbates inflammation by enhancing macrophage activation and ROS production, creating a vicious cycle of inflammation and oxidative stress (Figure 6).[112,113,115]

Chrysin pre-treatment significantly diminished MPO activity and reduced IFN-γ and IL-1β levels, demonstrating potent anti-inflammatory effects (Figure 5). These effects are mediated through inhibition of NF-κB signaling, a master regulator of inflammation.[90,91] Chrysin prevents the

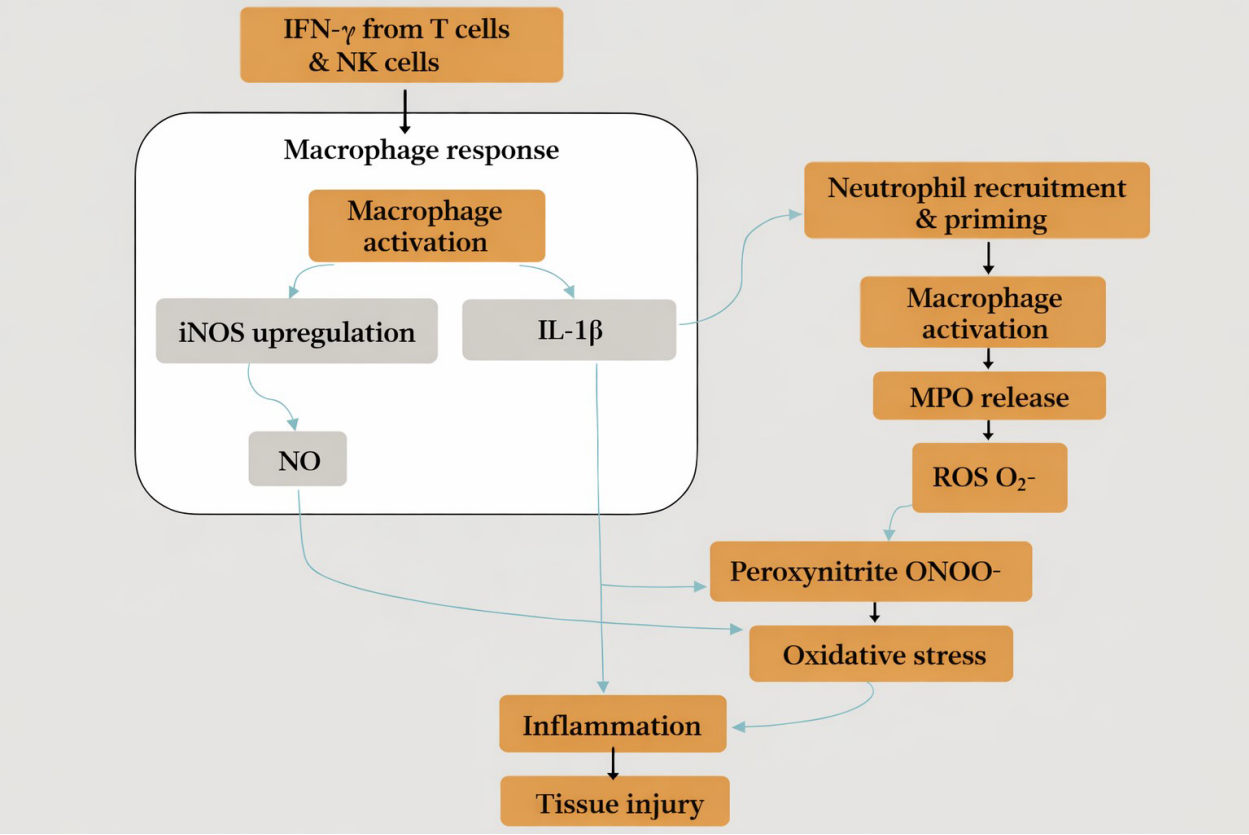


**Figure 6.** Schematic representation of the interplay between inflammatory mediators and oxidative stress pathways, illustrating how IFN-γ, IL-1β, iNOS-derived NO, and neutrophil-derived ROS converge to promote peroxynitrite formation, inflammation, and tissue injury. Adapted from Refs.[116–120]
Abbreviations: IFN: Interferon; IL: Interleukin; iNOS: Inducible nitric oxide synthase; MPO: Myeloperoxidase; NO: Nitric oxide; ROS: Reactive oxygen species.

degradation of inhibitor of κB, thereby retaining NF-κB in the cytoplasm and reducing the transcription of pro-inflammatory genes, including those encoding cytokines, chemokines, and adhesion molecules.[8,90,121,122] Additionally, the marked reduction in inflammatory mediators following chrysin pre-treatment suggests a pronounced anti-inflammatory effect. Previous studies have reported that chrysin attenuates inflammatory responses partly through inhibition of NLRP3 inflammasome activation and its downstream signaling cascade. The observed reductions in MPO activity, IFN-γ, and IL-1β are consistent with an attenuation of inflammatory responses that may involve this pathway.[89,91,123] The reduction in MPO activity indicates diminished neutrophil recruitment and activation, further attenuating tissue inflammation and oxidative damage.[124,125]

Chrysin's efficacy against PFOA-induced nephrotoxicity aligns with its reported protective effects in diverse toxin models, including cisplatin, gentamicin, and methotrexate.[2,3,6,72,126,127] The dose-dependent response observed in this study (25 and 50 mg/kg) mirrors pharmacokinetic studies noting chrysin's low oral bioavailability (~0.02%), which necessitates higher doses to achieve therapeutic tissue concentrations.[32,66,128] However, the absence of toxicity in the chrysin-only group reinforces its safety profile, a critical consideration for potential clinical translation.[3,66] The superior efficacy of the 50 mg/kg dose for most parameters, including ATPase restoration, antioxidant enhancement, and inflammatory suppression, underscores the importance of dose optimization in achieving chrysin's full therapeutic potential.[22,129]

Bioaccumulation of PFOA in renal tissues, driven by reabsorption mechanisms and resistance to degradation, exacerbates oxidative and inflammatory damage over time.[10,69,130] This persistent accumulation contributes to chronic renal injury and progressive functional decline, highlighting the need for effective interventions against long-term PFOA exposure. Chrysin's ability to

counteract these effects positions it as a promising natural countermeasure for persistent environmental pollutants, addressing significant gaps in current therapeutic strategies for chemical nephrotoxicity.[2,65,131] The bioaccumulative nature of PFOA, as highlighted in recent toxicokinetic models, prolongs its half-life and enhances its nephrotoxic potential, making interventions like chrysin critically important for populations with chronic environmental exposure.

The biomarkers assessed in this study are interconnected in a complex pathological network amplified by PFOA toxicity, as illustrated in Figure 6. Oxidative stress initiates inflammation through activation of redox-sensitive transcription factors such as NF-κB, while inflammatory cytokines further amplify ROS production through activation of neutrophils and macrophages.[112,113] This vicious cycle exacerbates cellular damage, leading to ATPase dysfunction and electrolyte imbalances, which in turn compromise renal function and exacerbate injury. Chrysin's multifaceted action disrupts this cycle at multiple points simultaneously: its antioxidant properties reduce oxidative stress, which in turn dampens inflammation and preserves ATPase function.[89,90] The restoration of ion homeostasis supports cellular energy metabolism and integrity, while anti-inflammatory effects prevent immune-mediated damage and tissue remodeling.[2,8] This synergistic mechanism highlights chrysin's potential as a comprehensive nephroprotective agent against environmental toxins such as PFOA, which exert complex mechanisms of toxicity.

Nevertheless, the present study has several limitations that should be acknowledged. First, the relatively small sample size ($n$ = 5 per group) and the short experimental duration (14 days) may limit the generalizability of the findings, particularly under chronic exposure conditions. Given the bioaccumulative nature of PFOA and its association with progressive renal dysfunction, the present findings should be interpreted within the context of an acute experimental model.[10,64] Second, although significant improvements in renal function, oxidative stress, inflammatory biomarkers, electrolyte homeostasis, and membrane-bound ATPase activities were observed, histopathological evaluation of kidney tissues was not performed. Consequently, the biochemical findings could not be directly correlated with structural renal alterations. Furthermore, although previous studies have implicated Nrf2/HO-1–mediated antioxidant signaling, NF-κB, and NLRP3 inflammasome modulation in the nephroprotective actions of chrysin, these molecular pathways were not directly evaluated in the present study using techniques such as Western blotting, quantitative polymerase chain reaction, or target-specific enzyme-linked immunosorbent assay. Therefore, the proposed involvement of these signaling pathways is based on published evidence and the biochemical responses observed in the present study rather than direct molecular confirmation. Another important limitation is the poor oral bioavailability of chrysin, largely attributable to its limited aqueous solubility and extensive first-pass metabolism, which may hinder its clinical translation despite its promising pharmacological properties.[66,67] Finally, as with most preclinical investigations, the use of an animal model cannot fully recapitulate the metabolic variability, genetic diversity, and complex environmental exposures encountered in humans; therefore, caution should be exercised when extrapolating these findings to clinical settings.

Future studies should employ larger experimental cohorts and extended treatment durations to evaluate the long-term nephroprotective efficacy and safety of chrysin under chronic PFOA exposure. Incorporating both qualitative and quantitative histopathological analyses, including tubular injury scoring and morphometric assessments, together with molecular investigations of oxidative stress, inflammatory, apoptotic, and cytoprotective signaling pathways, particularly Nrf2/HO-1, NF-κB, and NLRP3 inflammasome signaling, would provide stronger mechanistic evidence supporting the biochemical findings of the present study. Considering the pharmacokinetic limitations of chrysin, future research should also investigate advanced drug-delivery strategies, including nanoencapsulation, liposomes, phospholipid complexes, structural modification, and co-administration with bioavailability enhancers such as piperine, to improve its systemic bioavailability and therapeutic efficacy.[66] Ultimately, comprehensive pharmacokinetic, toxicological, and well-designed clinical studies are required to establish the long-term safety, potential drug interactions, optimal dosing strategies, and therapeutic efficacy of chrysin in individuals chronically exposed to PFOA and other per- and polyfluoroalkyl substances. Despite these limitations, the present study provides compelling evidence supporting the nephroprotective potential of chrysin and establishes a solid foundation for future mechanistic, pharmacological, and translational research aimed at developing natural therapeutic interventions against per- and polyfluoroalkyl substance-induced nephrotoxicity.

## 5. Conclusion

Chrysin pre-treatment mitigated PFOA-induced renal injury in male Wistar rats in a dose-dependent manner, with the higher dose conferring greater nephroprotection. These protective effects were associated with attenuation of oxidative stress, modulation of inflammatory

responses, restoration of membrane-bound ATPase activities, normalization of electrolyte homeostasis, and preservation of renal function. Although the underlying molecular pathways were not directly investigated in the present study, the findings provide strong biochemical evidence supporting the nephroprotective potential of chrysin against PFOA-induced kidney dysfunction. Future studies incorporating detailed molecular analyses, histopathological evaluation, pharmacokinetic assessment, and long-term exposure models are warranted to further elucidate its mechanisms of action and facilitate its potential translational application.

## Acknowledgments

None.

## Funding

None.

## Conflict of interest

The authors declare that there are no conflicts of interest regarding the conduct of this study or its publication.

## Author contributions

*Conceptualization:* Adeoye B. Awolesi
*Data curation:* Adeoye B. Awolesi, Tomisin M. Koledoye, Rereloluwa M. Adesina
*Formal analysis:* Adeoye B. Awolesi, Stephen A. Praise, Tomisin M. Koledoye
*Investigation:* Adeoye B. Awolesi, Stephen A. Praise, Tomisin M. Koledoye
*Methodology:* Adeoye B. Awolesi, Tomisin M. Koledoye
*Project administration:* Adeoye B. Awolesi, Tomisin M. Koledoye
*Resources:* Adeoye B. Awolesi
*Software:* Adeoye B. Awolesi, Rereloluwa M. Adesina
*Supervision:* Adeoye B. Awolesi
*Validation:* Tomisin M. Koledoye
*Visualization:* Adeoye B. Awolesi, Tomisin M. Koledoye, Rereloluwa M. Adesina
*Writing–original draft:* Adeoye B. Awolesi, Tomisin M. Koledoye
*Writing–review and editing:* Adeoye B. Awolesi, Kikelomo C. Omoniyi, Stephen A. Praise
All authors have read and approved the final version of the manuscript.

## Ethics approval and consent to participate

All animals were handled and cared for in accordance with the ARRIVE guidelines. Ethical approval for this study was obtained from the Federal University of Agriculture, Abeokuta Ethical Committee (Approval No. FUNAAB/COLBIOS/BCH/UG/20191153).

## Consent for publication

Not applicable.

## Availability of data

Data are available from the corresponding author upon request.

## Further disclosure

No artificial intelligence tools were used in the writing, analysis, interpretation, or preparation of this manuscript.

## References

1. Mohamed HK, Mobasher MA, Ebiya RA, *et al.* Anti-inflammatory, anti-apoptotic, and antioxidant roles of honey, royal jelly, and propolis in suppressing nephrotoxicity induced by doxorubicin in male albino rats. *Antioxidants*. 2022;11(5):1029.

   doi: 10.3390/antiox11051029

2. Pingili RB, Pawar AK, Challa SR, *et al.* A comprehensive review on hepatoprotective and nephroprotective activities of chrysin against various drugs and toxic agents. *Chem-Biol Interact*. 2019;308:51-60.

   doi: 10.1016/j.cbi.2019.05.010

3. Samarghandian S, Farkhondeh T, Azimi-Nezhad M. Protective Effects of Chrysin Against Drugs and Toxic Agents. *Dose-Response*. 2017;15(2):155932581771178.

   doi: 10.1177/1559325817711782

4. Ujah GA, Ofutet EO, Ukam CIO, *et al.* Protective effect of tert-butylhydroquinone against cisplatin-induced hepatorenal injury via modulating oxidative stress, inflammation, and apoptosis. *Arch Physiol Biochem*. 2024;130(6):951-961.

   doi: 10.1080/13813455.2024.2376812

5. Zhang X, Qian J, Wei B, *et al.* Flavonoids as modulators of Nrf2 signaling pathway in alleviating cisplatin-induced organ toxicity. *Yangtze Med*. 2025;09(01):52–77.

   doi: 10.4236/ym.2025.91006

6. Ali BH, Adham SA, Al Za'abi M, *et al.* Ameliorative effect of chrysin on adenine-induced chronic kidney disease in rats. *PloS ONE*. 2015;10(4):e0125285.

   doi: 10.1371/journal.pone.0125285

7. Chen M, Li J, Liu X, *et al.* Chrysin prevents lipopolysaccharide-induced acute lung injury in mice by suppressing the IRE1α/TXNIP/NLRP3 pathway. *Pulm Pharmacol Ther*. 2021;68:102018.

   doi: 10.1016/j.pupt.2021.102018

8. Nagavally RR, Sunilkumar S, Akhtar M, *et al.* Chrysin ameliorates Cyclosporine-A-induced renal fibrosis by inhibiting TGF-β1-induced epithelial–Mesenchymal Transition. *Int J Mol Sci*. 2021;22(19):10252.

doi: 10.3390/ijms221910252

9. Barnett LM, Cummings BS. Nephrotoxicity and renal pathophysiology: a contemporary perspective. *Toxicol Sci*. 2018;164(2):379-390.

doi: 10.1093/toxsci/kfy159

10. Liu D, Yan S, Wang P, *et al.* Perfluorooctanoic acid (PFOA) exposure in relation to the kidneys: A review of current available literature. *Front Physiol*. 2023;14.

doi: 10.3389/fphys.2023.1103141

11. Fenton SE, Ducatman A, Boobis A, DeWitt JC, Lau C, Ng C, *et al.* Per-and polyfluoroalkyl substance toxicity and human health review: Current state of knowledge and strategies for informing future research. *Environ Toxicol Chem*. 2020;40(3):606-630.

doi: 10.1002/etc.4890

12. Rashid F, Ramakrishnan A, Fields C, *et al.* Acute PFOA exposure promotes epigenomic alterations in mouse kidney tissues. *Toxicol Rep*. 2020;7:125-132.

doi: 10.1016/j.toxrep.2019.12.010

13. Ma X, Ren X, Zhang X, *et al.* Rutin ameliorate PFOA induced renal damage by reducing oxidative stress and improving lipid metabolism. *J Nutr Biochem*. 2024;123:109501.

doi: 10.1016/j.jnutbio.2023.109501

14. Zou W, Liu W, Yang B, *et al.* Quercetin protects against perfluorooctanoic acid-induced liver injury by attenuating oxidative stress and inflammatory response in mice. *Int Immunopharmacol*. 2015;28(1):129-135.

doi: 10.1016/j.intimp.2015.05.043

15. Mohany M, Ahmed MM, Al-Rejaie SS. Molecular mechanistic pathways targeted by natural antioxidants in the prevention and treatment of chronic kidney disease. *Antioxidants*. 2021;11(1):15.

doi: 10.3390/antiox11010015

16. Sarmah D, Sengupta R. A Review on the Role of Phytoconstituents Chrysin on the Protective Effecton Liver and Kidney. *CDDT*. 2024;21(1).

doi: 10.2174/0115701638242317231018144944

17. Kay AG, Rooney P, Kearney J, *et al.* Evaluation of DMSO transport in human articular cartilage: Vehicle solutions and effects on cell function. *Cryo Lett*. 2015;36(3):187-194. https://pubmed.ncbi.nlm.nih.gov/26510337/

18. Santos NC, Figueira-Coelho J, Martins-Silva J, *et al.* Multidisciplinary utilization of dimethyl sulfoxide: pharmacological, cellular, and molecular aspects. *Biochem Pharmacol*. 2003;65(7):1035-1041.

doi: 10.1016/S0006-2952(03)00002-9

19. Ortiz MI, Cariño-Cortés R, Fernández-Martínez E, *et al.* Peripheral Antinociception Induced by Carvacrol in the Formalin Test Involves the Opioid Receptor-NO-cGMP-K+ Channel Pathway. *Metabolites*. 2025;15(5):314.

doi: 10.3390/metabo15050314

20. Cheung C, Loy S, Li GX, *et al.* Rapid induction of colon carcinogenesis in CYP1A-humanized mice by 2-amino-1-methyl-6-phenylimidazo[4,5-b]pyridine and dextran sodium sulfate. *Carcinogenesis*. 2010;32(2):233-239.

doi: 10.1093/carcin/bgq235

21. Crebelli R, Caiola S, Conti L, *et al.* Can sustained exposure to PFAS trigger a genotoxic response? A comprehensive genotoxicity assessment in mice after subacute oral administration of PFOA and PFBA. *Regul Toxicol Pharmacol*. 2019;106:169-177.

doi: 10.1016/j.yrtph.2019.05.005

22. Eldutar E, Kandemir FM, Kucukler S, *et al.* Restorative effects of Chrysin pre-treatment on oxidant–antioxidant status, inflammatory cytokine production, and apoptotic and autophagic markers in acute paracetamol-induced hepatotoxicity in rats: An experimental and biochemical study. *J Biochem Molecular Tox*. 2017;31(11).

doi: 10.1002/jbt.21960

23. Kseibati MO, Sharawy MH, Salem HA. Chrysin mitigates bleomycin-induced pulmonary fibrosis in rats through regulating inflammation, oxidative stress, and hypoxia. *Int Immunopharmacol*. 2020;89:107011.

doi: 10.1016/j.intimp.2020.107011

24. Renuka M, Vijayakumar N, Ramakrishnan A. Chrysin, a flavonoid attenuates histological changes of hyperammonemic rats: A dose dependent study. *Biomed Pharmacother*. 2016;82:345-354.

doi: 10.1016/j.biopha.2016.05.013

25. Yao Y, Chen L, Xiao J, *et al.* Chrysin Protects against Focal Cerebral Ischemia/Reperfusion Injury in Mice through Attenuation of Oxidative Stress and Inflammation. *Int J Mol Sci*. 2014;15(11):20913-20926.

doi: 10.3390/ijms151120913

26. Zanoli P, Avallone R, Baraldi M. Behavioral characterisation of the flavonoids apigenin and chrysin. *Fitoterapia*. 2000;71:S117-S123.

doi: 10.1016/S0367-326X(00)00186-6

27. Albus U. Guide for the Care and Use of Laboratory Animals (8th edn). *Lab Anim*. 2012;46(3):267-268.

doi: 10.1258/la.2012.150312

28. Percie du Sert N, Hurst V, Ahluwalia A, *et al.* The ARRIVE

guidelines 2.0: Updated guidelines for reporting animal research. *Exp Physiol*. 2020;105(9):1459-1466.

doi: 10.1113/EP088870

29. Jacob SW, Herschler R. Pharmacology of DMSO. *Cryobiology*. 1986;23(1):14–27.

doi: 10.1016/0011-2240(86)90014-3

30. Panaretakis T, Shabalina IG, Grandér D, *et al.* Reactive Oxygen Species and Mitochondria Mediate the Induction of Apoptosis in Human Hepatoma HepG2 Cells by the Rodent Peroxisome Proliferator and Hepatocarcinogen, Perfluorooctanoic Acid. *Toxicol Appl Pharmacol*. 2001;173(1):56-64.

doi: 10.1006/taap.2001.9159

31. Tur R, Betelu S, Rodrigues R, *et al.* Optimization of experimental conditions of PFOA defluorination using DMSO/NaOH mixture. In: *18th International Symposium on Persistent Toxic Substances and Health (ISPTS-2024)*. 2024. https://brgm.hal.science/hal-04648668/

32. Walle T, Otake Y, Brubaker JA, *et al.* Disposition and metabolism of the flavonoid chrysin in normal volunteers. *Brit J Clin Pharma*. 2001;51(2):143-146.

doi: 10.1111/j.1365-2125.2001.01317.x

33. Cui L, Zhou QF, Liao CY, *et al.* Studies on the Toxicological Effects of PFOA and PFOS on Rats Using Histological Observation and Chemical Analysis. *Arch Environ Contam Toxicol.* 2008;56(2):338-349.

doi: 10.1007/s00244-008-9194-6

34. Yahia D, El-Nasser MA, Abedel-Latif M, *et al.* Effects of perfluorooctanoic acid (PFOA) exposure to pregnant mice on reproduction. *J Toxicol Sci*. 2010;35(4):527-533.

doi: 10.2131/jts.35.527

35. Yang B, Zou W, Hu Z, *et al.* Involvement of oxidative stress and inflammation in liver injury caused by perfluorooctanoic acid exposure in mice. *BioMed Res Int*. 2014;2014:1-7.

doi: 10.1155/2014/409837

36. James AS, Onunkwor BO, Akinseye VO, *et al.* Cashew nut-supplemented diet on testicular injury in rats exposed to sub-acute alcohol. *Pharmacol Res-Rep*. 2023;1:100001.

doi: 10.1016/j.prerep.2024.100001

37. Gad SB, Zaghloul DM. Beneficial Effects of Green Tea Extract on Liver and Kidney Functions, Ultrastructure, Lipid Profile and Hematological Parameters in Aged Male Rats. *Glob Vet*. 2013;11(2):191-205.

doi: 10.5829/idosi.gv.2013.11.2.7472

38. Hasim H, Mohamed Salam SKN, Rao PV, *et al.* Tualang honey-mediated silver nanoparticles attenuate hippocampal oxidative stress in kainic acid-induced male rats. *Biomed Res Ther*. 2022;9(12):5465-5475.

doi: 10.15419/bmrat.v9i12.785

39. Baghirova S, Hughes BG, Hendzel MJ, *et al.* Sequential fractionation and isolation of subcellular proteins from tissue or cultured cells. *MethodsX*. 2015;2:440-445.

doi: 10.1016/j.mex.2015.11.001

40. Blalock TD, Varela JC, Gowda S, *et al.* Ischemic skin wound healing models in rats. *Wounds*. 2001;13(1):35-44.

41. Wang Z, Zhang S, Li X, *et al.* Anti-aging potential of Limosilactobacillus fermentum F-B9-1-2 extracellular vesicles in D-galactose–induced cellular and organ senescence. *Sci Rep*. 2026;16(1).

doi: 10.1038/s41598-026-43553-1

42. Lowry O, Rosebrough N, Farr AL, Randall RJ. Protein measurement with the Folin phenol reagent. *J Biol Chem*. 1951;193(1):265-275.

doi: 10.1016/S0021-9258(19)52451-6

43. Chou SC, Goldstein A. Chromogenic groupings in the Lowry protein determination. *Biochem J.* 1960;75(1):109-115.

doi: 10.1042/bj0750109

44. Holmes RS, Scopes RK. Immunochemical Homologies among Vertebrate Lactate-Dehydrogenase Isozymes. *Eur J Biochem*. 1974;43(1):167-177.

doi: 10.1111/j.1432-1033.1974.tb03397.x

45. Al-Jassabi S. Purification and Kinetic Properties of Skeletal Muscle Lactate Dehydrogenase from the Lizard Agama stellio stellio. *Biochemistry*. 2002;67(7):786-789.

doi: 10.1023/A:1016300808378

46. Hodges DM, DeLong JM, Forney CF, *et al.* Improving the thiobarbituric acid-reactive-substances assay for estimating lipid peroxidation in plant tissues containing anthocyanin and other interfering compounds. *Planta*. 1999;207(4):604-611.

doi: 10.1007/s004250050524

47. Buege JA, Aust SD. [30] Microsomal lipid peroxidation. In: *Methods in Enzymology*. Elsevier; 1978:302-310.

doi: 10.1016/S0076-6879(78)52032-6

48. Ellman GL. Tissue sulfhydryl groups. *Archives of Arch Biochem Biophys*. 1959;82(1):70-77.

doi: 10.1016/0003-9861(59)90090-6

49. Ellis HR. On'tissue sulfhydryl groups' by George L. Ellman. *Arch Biochem Biophys*. 2022;726:109174.

doi: 10.1016/j.abb.2022.109174

50. Sun Y, Oberley LW, Li Y. A simple method for clinical assay of superoxide dismutase. *Clin Chem*. 1988;34(3):497-500.

doi: 10.1093/clinchem/34.3.497

51. Marklund S, Marklund G. Involvement of the superoxide anion radical in the autoxidation of pyrogallol and a convenient assay for superoxide dismutase. *Eur J Biochem*. 1974;47(3):469-474.

doi: 10.1111/j.1432-1033.1974.tb03714.x

52. Shangari N, O'Brien PJ. Catalase Activity Assays. *CP Toxicol*. 2006;27(1).

doi: 10.1002/0471140856.tx0707s27

53. Rotruck JT, Pope AL, Ganther HE, *et al.* Selenium: biochemical role as a component of glutathione peroxidase. *Nutr Rev*. 1980;38(8):280–3.

doi: 10.1111/j.1753-4887.1980.tb05961.x

54. Habig WH, Pabst MJ, Jakoby WB. Glutathione S-Transferases. *J Biol Chem*. 1974;249(22):7130-7139.

doi: 10.1016/S0021-9258(19)42083-8

55. Tew KD, Ronai Z. GST function in drug and stress response. *Drug Resist Updates*. 1999;2(3):143-147.

doi: 10.1054/drup.1999.0086

56. Prieto P, Pineda M, Aguilar M. Spectrophotometric quantitation of antioxidant capacity through the formation of a phosphomolybdenum complex: specific application to the determination of vitamin E. *Anal Biochem*. 1999;269(2):337-341.

doi: 10.1006/abio.1999.4019

57. Tsakiris S, Deliconstantinos G. Influence of phosphatidylserine on (Na++ K+)-stimulated ATPase and acetylcholinesterase activities of dog brain synaptosomal plasma membranes. *Biochem J*. 1984;220(1):301-307.

doi: 10.1042/bj2200301

58. Katewa SD, Katyare SS. A simplified method for inorganic phosphate determination and its application for phosphate analysis in enzyme assays. *Anal Biochem*. 2003;323(2):180-187.

doi: 10.1016/j.ab.2003.08.024

59. Hanahan DJ, Ekholm JE. [15] The preparation of red cell ghosts (membranes). In: *Methods in Enzymology*. Elsevier; 1974:168-172.

doi: 10.1016/0076-6879(74)31018-X

60. Green LC, Wagner DA, Glogowski J, *et al.* Analysis of nitrate, nitrite, and [15N] nitrate in biological fluids. *Anal Biochem*. 1982;126(1):131-138.

doi: 10.1016/0003-2697(82)90118-X

61. Akamo AJ, Ojelabi AO, Akamo NM, *et al.* Hesperetin-7-rutinoside mitigates erythrocyte dyslipidemia and oxidative stress induced by dichlorvos. *J Hazard Mater Adv.* 2024;16:100495.

doi: 10.1016/j.hazadv.2024.100495

62. Privat C, Lantoine F, Bedioui F, *et al.* Nitric oxide production by endothelial cells: Comparison of three methods of quantification. *Life Sci*. 1997;61(12):1193-1202.

doi: 10.1016/S0024-3205(97)00661-9

63. Hasmann A, Wehrschuetz-Sigl E, Marold A, *et al.* Analysis of myeloperoxidase activity in wound fluids as a marker of infection. *Ann Clin Biochem*. 2013;50(3):245-254.

doi: 10.1258/acb.2011.010249

64. Bonato M, Corrà F, Bellio M, *et al.* PFAS environmental pollution and antioxidant responses: an overview of the impact on human field. *Int J Environ Res Public Health*. 2020;17(21):8020.

doi: 10.3390/ijerph17218020

65. Mani R, Natesan V. Chrysin: Sources, beneficial pharmacological activities, and molecular mechanism of action. *Phytochemistry*. 2018;145:187-196.

doi: 10.1016/j.phytochem.2017.09.016

66. Gao S, Siddiqui N, Etim I, *et al.* Developing nutritional component chrysin as a therapeutic agent: Bioavailability and pharmacokinetics consideration, and ADME mechanisms. *Biomed Pharmacother*. 2021;142:112080.

doi: 10.1016/j.biopha.2021.112080

67. Stompor-Gorący M, Bajek-Bil A, Machaczka M. Chrysin: Perspectives on Contemporary Status and Future Possibilities as Pro-Health Agent. *Nutrients*. 2021;13(6):2038.

doi: 10.3390/nu13062038

68. Kurkiewicz M, Moździerz A, Rzepecka-Stojko A, *et al.* Chrysin: A comprehensive review of its pharmacological properties and therapeutic potential. *Pharmaceuticals*. 2025;18(8):1162.

doi: 10.3390/ph18081162

69. Boston C, Keck S, Naperala A, *et al.* The evolution of PFAS epidemiology: new scientific developments call into question alleged "probable links" between PFOA and kidney cancer and thyroid disease. *Front Public Health*. 2025;13.

doi: 10.3389/fpubh.2025.1532277

70. Wang L, Sun W, Ma X, *et al.* Perfluorooctanoic acid (PFOA) exposure induces renal filtration and reabsorption disorders via down-regulation of aquaporins. *Toxicol Lett*. 2024;392:22-35.

doi: 10.1016/j.toxlet.2023.12.003

71. Gorelik Y, Abassi Z, Bloch-Isenberg N, *et al.* Changing serum creatinine in the detection of acute renal failure and recovery following radiocontrast studies among acutely ill inpatients: reviewing insights regarding renal functional reserve gained by large-data analysis. *Pract Lab Med*. 2022;30:e00276.

doi: 10.1016/j.plabm.2022.e00276

72. Sultana S, Verma K, Khan R. Nephroprotective efficacy of

chrysin against cisplatin-induced toxicity via attenuation of oxidative stress. *J Pharm Pharmacol.* 2012;64(6):872-881.

doi: 10.1111/j.2042-7158.2012.01470.x

73. Ozoemena CL, Abireh IE, Katchy AU. Probing the Nephroprotective Potential of Chrysin against Methotrexate-Induced Tubulointerstitial Nephritis and Oxidative Damage. *Trop J Nat Product Res*. 2024;8(7).

doi: 10.26538/tjnpr/v8i7.30

74. Farhana A, Lappin SL. Biochemistry, Lactate Dehydrogenase. In: StatPearls. StatPearls Publishing; 2023. https://www.ncbi.nlm.nih.gov/books/NBK557536/

75. Udayakumar S. Vacuolation: A Novel Biomarker of Environmental Pollutant PFOA Induced Human Renal Proximal Tubular Cell Injury. *Int J High School Res*. 2025;7(4):9-12.

doi: 10.36838/v7i4.2

76. Xiao X, Zhang J, Lang Y, *et al.* Associations of lactate dehydrogenase with risk of renal outcomes and cardiovascular mortality in individuals with diabetic kidney disease. *Diabetes Res Clini Pract*. 2023;203:110838.

doi: 10.1016/j.diabres.2023.110838

77. Tahir M, Sultana S. Chrysin modulates ethanol metabolism in Wistar rats: a promising role against organ toxicities. *Alcohol Alcohol*. 2011;46(4):383-392.

doi: 10.1093/alcalc/agr038

78. Adeva-Andany M, López-Ojén M, Funcasta-Calderón R, *et al.* Comprehensive review on lactate metabolism in human health. *Mitochondrion*. 2014;17:76-100.

doi: 10.1016/j.mito.2014.05.007

79. Rogatzki MJ, Ferguson BS, Goodwin ML, *et al.* Lactate is always the end product of glycolysis. *Front Neurosci*. 2015;9.

doi: 10.3389/fnins.2015.00022

80. Starnes HM, Rock KD, Jackson TW, *et al.* A critical review and meta-analysis of impacts of per-and polyfluorinated substances on the brain and behavior. *Front Toxicol*. 2022;4.

doi: 10.3389/ftox.2022.881584

81. Palmer BF, Clegg DJ. Physiology and pathophysiology of potassium homeostasis. *Adv Physiol Ed*. 2016;40(4):480-490.

doi: 10.1152/advan.00121.2016

82. Zhang X, Flaws JA, Spinella MJ, *et al.* The Relationship between Typical Environmental Endocrine Disruptors and Kidney Disease. *Toxics*. 2022;11(1):32.

doi: 10.3390/toxics11010032

83. Alexander RT, Dimke H. Effect of diuretics on renal tubular transport of calcium and magnesium. *Am J Physiol-Renal Physiol*. 2017;312(6):F998-F1015.

doi: 10.1152/ajprenal.00032.2017

84. Yadav S, Yadav J, Kumar S, *et al.* Metabolism of Macro-elements (Calcium, Magnesium, Sodium, Potassium, Chloride and Phosphorus) and Associated Disorders. In: *Clinical Applications of Biomolecules in Disease Diagnosis*. Springer Nature Singapore; 2024:177-203.

doi: 10.1007/978-981-97-4723-8_8

85. Chandra P, Pathak R, Sachan N. Chrysin: Chemistry, Occurrence, Pharmacokinetics, Toxicity, Molecular Targets, and Medicinal Properties of a Naturally Occurring Flavone. *CBC*. 2025;21(8).

doi: 10.2174/0115734072341901241121185020

86. Campos HM, da Costa M, da Silva Moreira LK, *et al.* Protective effects of chrysin against the neurotoxicity induced by aluminium: In vitro and in vivo studies. *Toxicology*. 2022;465:153033.

doi: 10.1016/j.tox.2021.153033

87. Alharthy SA, Hardej D. The role of transcription factor Nrf2 in the toxicity of perfluorooctane sulfonate (PFOS) and perfluorooctanoic acid (PFOA) in C57BL/6 mouse astrocytes. *Environ Toxicol Pharmacol*. 2021;86:103652.

doi: 10.1016/j.etap.2021.103652

88. Georgiou-Siafis SK, Tsiftsoglou AS. The key role of GSH in keeping the redox balance in mammalian cells: mechanisms and significance of GSH in detoxification via formation of conjugates. *Antioxidants*. 2023;12(11):1953.

doi: 10.3390/antiox12111953

89. Huang CS, Lii CK, Lin AH, *et al.* Protection by chrysin, apigenin, and luteolin against oxidative stress is mediated by the Nrf2-dependent up-regulation of heme oxygenase 1 and glutamate cysteine ligase in rat primary hepatocytes. *Arch Toxicol*. 2012;87(1):167-178.

doi: 10.1007/s00204-012-0913-4

90. Zeinali M, Rezaee SA, Hosseinzadeh H. An overview on immunoregulatory and anti-inflammatory properties of chrysin and flavonoids substances. *Biomed Pharmacother*. 2017;92:998-1009.

doi: 10.1016/j.biopha.2017.06.003

91. Rehman MU, Tahir M, Khan AQ, *et al.* Chrysin suppresses renal carcinogenesis via amelioration of hyperproliferation, oxidative stress and inflammation: Plausible role of NF-κB. *Toxicol Lett*. 2013;216(2-3):146-158.

doi: 10.1016/j.toxlet.2012.11.013

92. Talebi M, Talebi M, Farkhondeh T, *et al.* An updated review on the versatile role of chrysin in neurological diseases: Chemistry, pharmacology, and drug delivery approaches. *Biomed Pharmacother*. 2021;141:111906.

doi: 10.1016/j.biopha.2021.111906

93. Gupta S, Finelli R, Agarwal A, *et al.* Total antioxidant capacity—Relevance, methods and clinical implications.

*Andrologia*. 2020;53(2).

doi: 10.1111/and.13624

94. Ji L, Chauhan A, Brown WT, *et al.* Increased activities of Na+/K+-ATPase and Ca2+/Mg2+-ATPase in the frontal cortex and cerebellum of autistic individuals. *Life Sci*. 2009;85(23-26):788-793.

doi: 10.1016/j.lfs.2009.10.008

95. Scheiner-Bobis G. Ion-transporting ATPases as ion channels. *Naunyn-Schmiedeberg's Arc Pharmacol*. 1998;357(5):477-482.

96. Clausen MJV, Poulsen H. Sodium/Potassium Homeostasis in the Cell. In: *Metal Ions in Life Sciences*. Springer Netherlands; 2012:41-67.

doi: 10.1007/978-94-007-5561-1_3

97. Polak-Jonkisz D, Zwolińska D, Purzyc L, *et al.* Ca2+-Mg2+-dependent ATP-ase activity and calcium homeostasis in children with chronic kidney disease. *Pediatr Nephrol*. 2007;22(3):414-419.

doi: 10.1007/s00467-006-0329-6

98. Gielecińska A, Kciuk M, Kontek R. The Impact of Calcium Overload on Cellular Processes: Exploring Calcicoptosis and Its Therapeutic Potential in Cancer. *Int J Mol Sci.* 2024;25(24):13727.

doi: 10.3390/ijms252413727

99. Lee D, Hong JH. Physiological Overview of the Potential Link between the UPS and Ca2+ Signaling. *Antioxidants*. 2022;11(5):997.

doi: 10.3390/antiox11050997

100. Poór M, Veres B, Jakus PB, *et al.* Flavonoid diosmetin increases ATP levels in kidney cells and relieves ATP depleting effect of ochratoxin A. *J Photochem Photobiol B: Biol*. 2014;132:1–9.

doi: 10.1016/j.jphotobiol.2014.01.016

101. Sabry HA, Zahra MM, Haredy SA, *et al.* Neuroprotective impacts of chrysin against clonazepam induced cognitive deficits in male rats. *J App Pharm Sc*. 2023;13(7):174-185.

doi: 10.7324/JAPS.2023.13885

102. Basini G, Bussolati S, Torcianti V, *et al.* Perfluorooctanoic acid (PFOA) induces redox status disruption in swine granulosa cells. *Vet Sci*. 2022;9(6):254.

doi: 10.3390/vetsci9060254

103. Laycock SK, Vogel T, Forfia PR, *et al.* Role of Nitric Oxide in the Control of Renal Oxygen Consumption and the Regulation of Chemical Work in the Kidney. *Circ Res*. 1998;82(12):1263-1271.

doi: 10.1161/01.RES.82.12.1263

104. Ratliff BB, Abdulmahdi W, Pawar R, *et al.* Oxidant Mechanisms in Renal Injury and Disease. *Antioxid Redox Signal*. 2016;25(3):119-146.

doi: 10.1089/ars.2016.6665

105. Shen ZH, Ye T, Chen B, *et al.* 5, 7-Dihydroxyflavone acts on eNOS to achieve hypotensive effects in spontaneously hypertensive rats. *Sci Rep*. 2025;15(1).

doi: 10.1038/s41598-024-84259-6

106. Xu H, Yu S, Lin C, *et al.* Roles of flavonoids in ischemic heart disease: Cardioprotective effects and mechanisms against myocardial ischemia and reperfusion injury. *Phytomedicine*. 2024;126:155409.

doi: 10.1016/j.phymed.2024.155409

107. Yuvaraj S, Ramprasath T, Saravanan B, *et al.* Chrysin attenuates high-fat-diet-induced myocardial oxidative stress via upregulating eNOS and Nrf2 target genes in rats. *Mol Cell Biochem*. 2021;476(7):2719-2727.

doi: 10.1007/s11010-021-04105-5

108. Kothari N, Keshari RS, Bogra J, *et al.* Increased myeloperoxidase enzyme activity in plasma is an indicator of inflammation and onset of sepsis. *J Crit Care*. 2011;26(4): 435.e1-435.e7.

doi: 10.1016/j.jcrc.2010.09.001

109. Qazi MR, Bogdanska J, Butenhoff JL, *et al.* High-dose, short-term exposure of mice to perfluorooctanesulfonate (PFOS) or perfluorooctanoate (PFOA) affects the number of circulating neutrophils differently, but enhances the inflammatory responses of macrophages to lipopolysaccharide (LPS) in a similar fashion. *Toxicology*. 2009;262(3):207-214.

doi: 10.1016/j.tox.2009.06.010

110. Wang LQ, Liu T, Yang S, *et al.* Perfluoroalkyl substance pollutants activate the innate immune system through the AIM2 inflammasome. *Nat Commun*. 2021;12(1).

doi: 10.1038/s41467-021-23201-0

111. Wu L, Hu Z, Luo X, *et al.* Itaconic Acid Alleviates Perfluorooctanoic Acid-Induced Oxidative Stress and Intestinal Damage by Regulating the Keap1/Nrf2/Ho-1 Pathway and Reshaping the Gut Microbiota. *Int J MolSci*. 2024;25(18):9826.

doi: 10.3390/ijms25189826

112. Liang L, Pan Y, Bin L, *et al.* Immunotoxicity mechanisms of perfluorinated compounds PFOA and PFOS. *Chemosphere*. 2022;291:132892.

doi: 10.1016/j.chemosphere.2021.132892

113. Zhang H, Fang W, Wang D, *et al.* The role of interleukin family in perfluorooctanoic acid (PFOA)-induced immunotoxicity. *J Hazard Mater*. 2014;280:552-560.

doi: 10.1016/j.jhazmat.2014.08.043

114. Qin Y, Gu T, Ling J, *et al.* PFOS facilitates liver inflammation and steatosis: An involvement of NLRP3 inflammasome-

mediated hepatocyte pyroptosis. *J Appl Toxicol*. 2022;42(5):806-817.

doi: 10.1002/jat.4258

115. Schroecksnadel K, Frick B, Winkler C, *et al.* Crucial role of interferon-γ and stimulated macrophages in cardiovascular disease. *Curr Vasc Pharmacol*. 2006;4(3):205-213.

doi: 10.2174/157016106777698379

116. Dubey S, Khan J, Alishlash AS, *et al.* The Cell with Many Faces: Lung Macrophage Plasticity and Function in Response to Environmental and Pathogenic Insults. *Physiol Rev*. 2026;106(3):1999-2055.

doi: 10.1152/physrev.00038.2025

117. Kumar S, Dikshit M. Nitric oxide: Regulation and function in neutrophil immune responses. *Antioxid Redox Signal*. 2024;40(16–18):998–1024.

doi: 10.1089/ars.2022.0220

118. Matsuzawa T, Kim BH, Shenoy AR, *et al.* IFN-γ elicits macrophage autophagy via the p38 MAPK signaling pathway. *J Immunol*. 2012;189(2):813-818.

doi: 10.4049/jimmunol.1102041

119. Akagha MJ, Georgolopoulos G, Martin D, *et al.* IFNγ shapes macrophage inflammatory responses by STAT1 isoform-specific epigenetic and transcriptional mechanisms. *BMC Genomics*. 2026;27(1).

doi: 10.1186/s12864-026-12601-5

120. Ivashkiv LB. IFNγ: signalling, epigenetics and roles in immunity, metabolism, disease and cancer immunotherapy. *Nat Rev Immunol*. 2018;18(9):545-558.

doi: 10.1038/s41577-018-0029-z

121. Li X, Huang Q, Ong CN, *et al.* Chrysin sensitizes tumor necrosis factor-α-induced apoptosis in human tumor cells via suppression of nuclear factor-kappaB. *Cancer Lett*. 2010;293(1):109-116.

doi: 10.1016/j.canlet.2010.01.002

122. Yeo H, Lee YH, Koh D, *et al.* Chrysin Inhibits NF-κB-Dependent CCL5 Transcription by Targeting IκB Kinase in the Atopic Dermatitis-Like Inflammatory Microenvironment. *Int J Mol Sci*. 2020;21(19):7348.

doi: 10.3390/ijms21197348

123. Liao T, Ding L, Wu P, *et al.* Chrysin Attenuates the NLRP3 Inflammasome Cascade to Reduce Synovitis and Pain in KOA Rats. *Drug Des Devel Ther*. 2020;14:3015-3027.

doi: 10.2147/DDDT.S261216

124. Chen S, Chen H, Du Q, *et al.* Targeting myeloperoxidase (MPO) mediated oxidative stress and inflammation for reducing brain ischemia injury: potential application of natural compounds. *Front Physiol*. 2020;11.

doi: 10.3389/fphys.2020.00433

125. Kim HJ, Wei Y, Wojtkiewicz GR, *et al.* Reducing myeloperoxidase activity decreases inflammation and increases cellular protection in ischemic stroke. *J Cereb Blood Flow Metab*. 2018;39(9):1864-1877.

doi: 10.1177/0271678X18771978

126. Albukhari TA, Bagadood RM, Bokhari BT, *et al.* Chrysin Attenuates Gentamicin-Induced Renal Injury in Rats Through Modulation of Oxidative Damage and Inflammation via Regulation of Nrf2/AKT and NF-kB/KIM-1 Pathways. *Biomedicines*. 2025;13(2):271.

doi: 10.3390/biomedicines13020271

127. Ali N, Rashid S, Nafees S, *et al.* Beneficial effects of Chrysin against Methotrexate-induced hepatotoxicity via attenuation of oxidative stress and apoptosis. *Mol Cell Biochem*. 2013;385(1–2):215-223.

doi: 10.1007/s11010-013-1830-4

128. Lin JH. Dose-dependent pharmacokinetics: Experimental observations and theoretical considerations. *Biopharm Drug Disp*. 1994;15(1):1-31.

doi: 10.1002/bdd.2510150102

129. Roshanravan B, Farkhondeh T, Darroudi M, *et al.* Protective Effect of Chrysin Against Chlorpyrifos-induced Hepatotoxicityin Rats: Biochemical and Histopathological Approaches in a Sub-chronicStudy. *CPB*. 2023;24(10):1291-1296.

doi: 10.2174/1389201024666221025094643

130. Greene CW, Bogdan AR, Goeden HM. A revised and improved toxicokinetic model to simulate serum concentrations of bioaccumulative PFAS. *J Environ Expo Assess*. 2024;3(2).

doi: 10.20517/jeea.2024.09

131. Garg A, Chaturvedi S. A Comprehensive Review on Chrysin: Emphasis on Molecular Targets, Pharmacological Actions and Bio-pharmaceutical Aspects. *CDT*. 2022;23(4):420-436.

doi: 10.2174/1389450122666210824141044